Short article

Cell Host & Microbe

A conserved antigen induces respiratory Th17-mediated broad serotype protection against pneumococcal superinfection

Graphical abstract

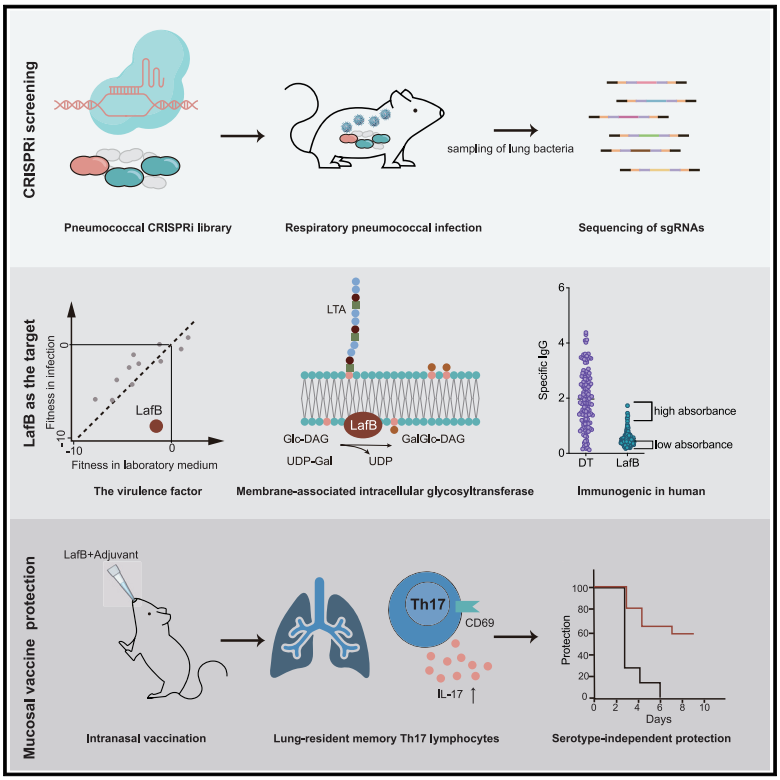

Highlights

- CRISPRi-seq in pneumococcal superinfection identified *lafB* as crucial for virulence
- LafB catalyzes the formation of a glycolipid important for cell wall homeostasis
- Intranasal vaccination with LafB protects against pneumococcal non-vaccine serotypes
- Nasal vaccine-induced protection depends on lung Th17 lymphocytes with TRM features

Authors

Xue Liu, Laurye Van Maele, Laura Matarazzo, ..., Victor Nizet, Jean-Claude Sirard, Jan-Willem Veening

Correspondence

jean-claude.sirard@inserm.fr (J.-C.S.), jan-willem.veening@unil.ch (J.-W.V.)

In brief

Liu et al. identify *lafB* as crucial for *Streptococcus pneumoniae* replication *in vivo* using CRISPRi-seq. Intranasal vaccination with flagellin-adjuvanted LafB induces lung Th7 lymphocytes that protect against superinfections with various pneumococcal serotypes in mice. Healthy individuals can elicit LafB-specific immune responses, suggesting that LafB is a universal, capsule-independent pneumococcal antigen.

Liu et al., 2024, Cell Host & Microbe *32*, 304–314
March 13, 2024
https://doi.org/10.1016/j.chom.2024.02.002

CellPress
OPEN ACCESS

Cell Host & Microbe

Short article

A conserved antigen induces respiratory Th17-mediated broad serotype protection against pneumococcal superinfection

Xue Liu,[1,2,6] Laurye Van Maele,[3,6] Laura Matarazzo,[3] Daphnée Soulard,[3] Vinicius Alves Duarte da Silva,[3] Vincent de Bakker,[2] Julien Dénéréaz,[2] Florian P. Bock,[2] Michael Taschner,[2] Jinzhao Ou,[1] Stephan Gruber,[2] Victor Nizet,[4,5] Jean-Claude Sirard,[3,*] and Jan-Willem Veening[2,4,7,*]

[1]Department of Pathogen Biology, Base for International Science and Technology Cooperation, Carson Cancer Stem Cell Vaccines R&D Center, International Cancer Center, Shenzhen University Medical School, Shenzhen 518060, China

[2]Department of Fundamental Microbiology, Faculty of Biology and Medicine, University of Lausanne, Biophore Building, CH-1015 Lausanne, Switzerland

[3]University of Lille, CNRS, Inserm, CHU Lille, Institut Pasteur Lille, U1019 - UMR 9017 - CIIL - Center for Infection and Immunity of Lille, 59000 Lille, France

[4]Department of Pediatrics, University of California, San Diego, La Jolla, CA, USA

[5]Skaggs School of Pharmacy and Pharmaceutical Sciences, University of California, San Diego, La Jolla, CA, USA

[6]These authors contributed equally

[7]Lead contact

*Correspondence: jean-claude.sirard@inserm.fr (J.-C.S.), jan-willem.veening@unil.ch (J.-W.V.)

https://doi.org/10.1016/j.chom.2024.02.002

SUMMARY

Several vaccines targeting bacterial pathogens show reduced efficacy upon concurrent viral infection, indicating that a new vaccinology approach is required. To identify antigens for the human pathogen *Streptococcus pneumoniae* that are effective following influenza infection, we performed CRISPRi-seq in a murine model of superinfection and identified the conserved *lafB* gene as crucial for virulence. We show that LafB is a membrane-associated, intracellular protein that catalyzes the formation of galactosyl-glucosyl-diacylglycerol, a glycolipid important for cell wall homeostasis. Respiratory vaccination with recombinant LafB, in contrast to subcutaneous vaccination, was highly protective against *S. pneumoniae* serotypes 2, 15A, and 24F in a murine model. In contrast to standard capsule-based vaccines, protection did not require LafB-specific antibodies but was dependent on airway $CD4^+$ T helper 17 cells. Healthy human individuals can elicit LafB-specific immune responses, indicating LafB antigenicity in humans. Collectively, these findings present a universal pneumococcal vaccine antigen that remains effective following influenza infection.

INTRODUCTION

Streptococcus pneumoniae is a leading cause of bacterial pneumonia and a major cause of death and disability in young children and aged or immunocompromised adults. Notoriously, *S. pneumoniae* proves particularly virulent in combination with antecedent influenza A virus infection. Such secondary pneumococcal infections, or superinfections, contribute significantly to excess morbidity and mortality in high-risk groups, as highlighted during the influenza pandemics of 1918, 1957, 1968, and 2009.[1–4]

Currently, pneumococcal vaccines are capsule polysaccharide (CPS)-based, such as Prevenar 13, which is composed of 13 CPSs conjugated to a carrier protein and Pneumovax, the pneumococcal polysaccharide vaccine (PPSV) that contains 23 CPSs.[5] Whereas both vaccines elicit CPS-specific antibodies, the conjugated vaccine induces T cell-dependent immunity, which elicits stronger and long-term antibodies.[6,7] While these vaccines are successful in reducing the burden of infections caused by 13–23 serotypes, they do not protect against invasive pneumococcal disease caused by non-vaccine serotypes.[8,9] There are more than 100 known serotypes of *S. pneumoniae*,[10] and serotype replacement and appearance of non-typeable clinical isolates reduce the efficacy of CPS-based vaccines.[11,12] To encompass a broader range of serotypes, recent vaccine developments include Prevenar 20, which targets 20 serotypes,[13] and Vaxneurance, covering 15 serotypes.[14] However, even with these advancements, only a subset of the serotypes are covered. Importantly, CPS-based vaccines provide poor protection during pneumococcal superinfection in mice.[15,16] How well CPS-based vaccines work in the context of superinfection is unclear from human vaccine studies.[17] What is clear is that influenza infection decreases pneumococcal clearance and increases lung injury even in PPSV-vaccinated mice.[16] Conversely, pneumococcal colonization may also impede mucosal responses to live attenuated influenza vaccine,

CellPress
OPEN ACCESS

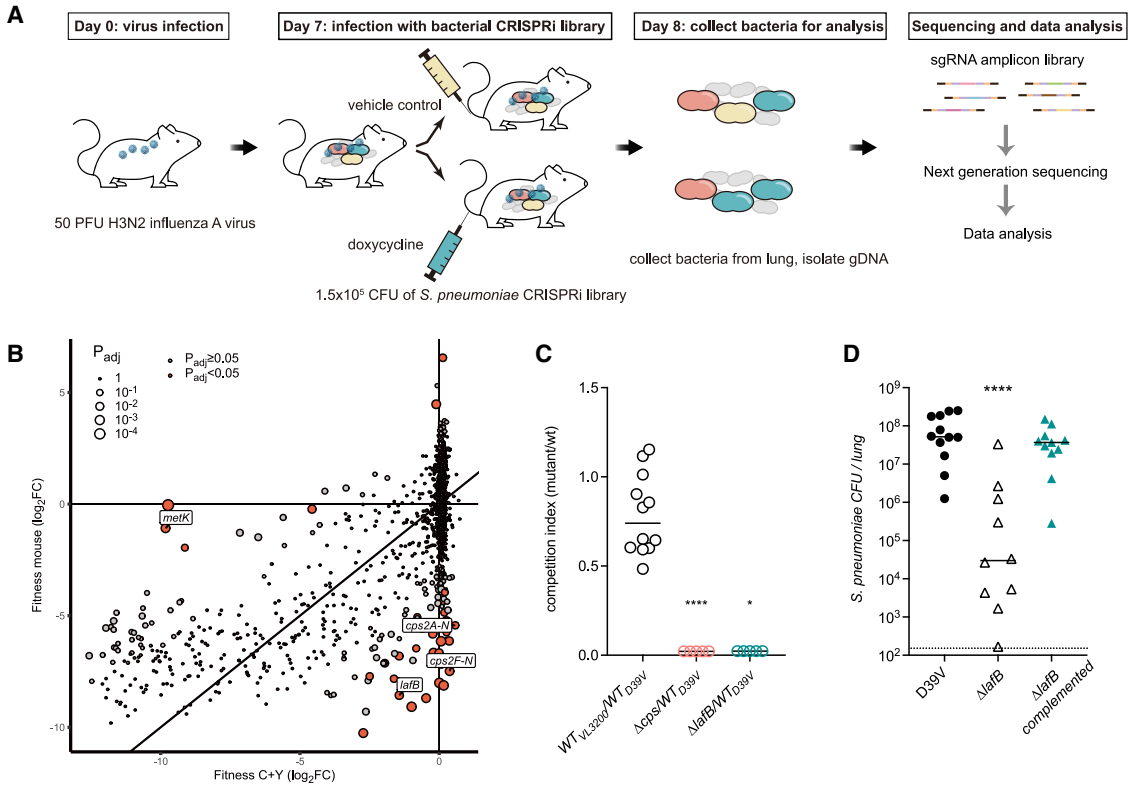

Figure 1. LafB is an essential virulence determinant

(A) Workflow of CRISPRi-seq using injected doxycycline. Mice (n = 5) were inoculated intranasally with the CRISPRi library.

(B) CRISPRi knockdown of the capsule operon (*cps2A-N*, *cps2F-N*) and *lafB* results in reduced fitness in mice, compared with *in vitro* (C + Y medium).

(C) Competition index of individual mutants, compared with wild-type (WT) D39V. Strain VL3200 is similar to WT but contains an erythromycin resistance marker at a neutral locus. Each datapoint represents the lung colony forming unit (CFU) count at day 8 of a single mouse infected with flu at day 0 and a ratio 1:1 of mutant and WT strain at day 7. Twelve animals were included in each group.

(D) The Δ*lafB* mutant was attenuated in establishing lung infection (11–12 mice per group). Ectopic expression of *lafB* complemented the phenotype. Kruskal-Wallis testing was used to compare groups.

including reduced production of nasal immunoglobulin A (IgA) and lung IgG in humans.[18]

Thus, there is an urgent need for an efficient vaccine that protects against any pneumococcal strain. A promising avenue for a universal, serotype-independent vaccine is in the use of immunogenic proteins as protective antigens.[5,19–27] So far, efforts have been focused on surface-exposed proteins as these might be directly recognized by opsonizing antibodies. However, surface-exposed proteins typically show significant strain-to-strain sequence variability because of antigenic variation.[28–30] To uncover universal antigens, an unbiased genome-wide vaccinology approach is required. Previous attempts have used transposon insertion sequencing (Tn-seq) to identify pneumococcal antigens.[31,32] While successful, these approaches identified non-essential genes encoding variable surface-exposed proteins that suffer from the limitations outlined above. Here, employing CRISPR interference (CRISPRi) that allows the interrogation of essential genes,[33] we searched specifically for conserved genes important for bacterial survival during superinfection. We show that one hit, lipoteichoic acid anchor formation protein B (LafB), a highly conserved membrane-associated protein, is important for cell wall homeostasis and crucial for virulence. Importantly, recombinant LafB provides broad T helper 17 (Th17) cell-specific protective immunity, paving the way for a universal, capsule-independent pneumococcal vaccine.

RESULTS

CRISPRi-seq identifies *S. pneumoniae* LafB as crucial for virulence during influenza superinfection

Using CRISPRi-seq of a genome-wide sgRNA library in mice fed doxycycline-containing food, we confirmed pneumococcal capsule as an important virulence factor during superinfection.[34] To precisely control *in vivo* dCas9 expression, doxycycline levels were optimized following intraperitoneal (i.p.) injection in mice. The *ex vivo* CRISPRi-based luciferase assay found that as little as 4 ng/ml doxycycline repressed luciferase transcription >15-fold (Figures S1A–S1D); i.p. injection of 5 mg/kg doxycycline adequately activated the pneumococcal CRISPRi system in the lung.

Next, mice were infected intranasally (i.n.) with H3N2 influenza virus, followed at day 7 by i.n. infection with the *S. pneumoniae* CRISPRi library. dCas9 was induced by doxycycline and compared with mock (vehicle) control (Figure 1A). CRISPRi-seq

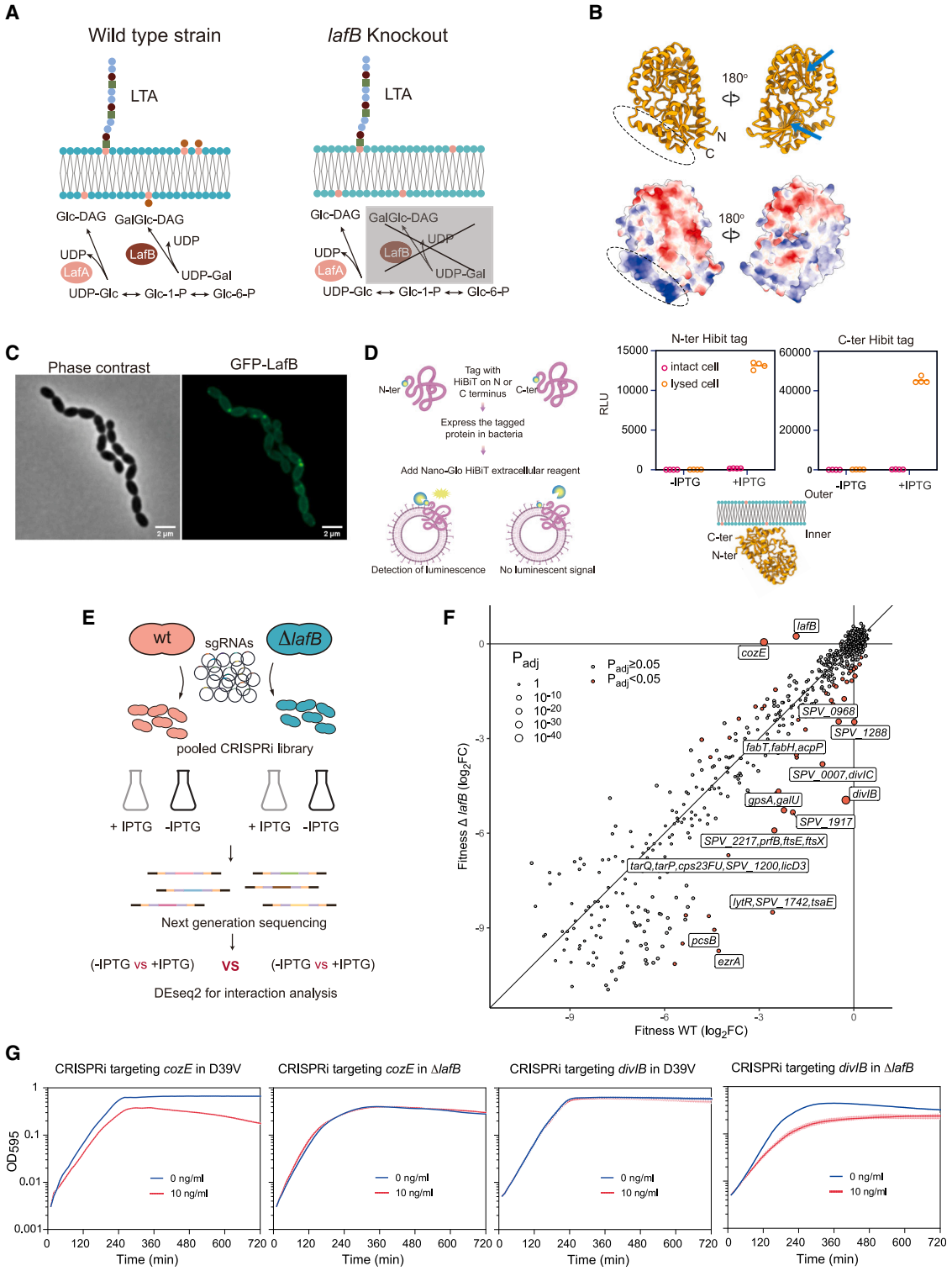

Figure 2. LafB is a membrane-associated galactosyl-glucosyl-diacylglycerol synthase with a pleiotropic role in cell wall homeostasis

(A) LafB is encoded in the same operon with LafA. LafA catalyzes the synthesis of glucosyl-diacylglycerol (Glc-DAG), which provides the anchor for lipoteichoic acids (LTA). LafB catalyzes the addition of galactose onto Glc-DAG synthesizing GalGlc-DAG (Figure S2).

(B) The predicted structure of LafB by RoseTTAFold. Negative and positive electrostatic potentials are colored red and blue, respectively. The two blue arrows point to the active units. No transmembrane domain was identified.

(C) Fluorescence microscopy analysis of GFP-LafB showed a membrane localization.

(legend continued on next page)

CellPress
OPEN ACCESS

confirmed the capsule operon as critical for pneumococcal virulence; in contrast, the *in vitro* essential gene *metK* was dispensable *in vivo*[34] (Figure 1B). To pinpoint conserved *S. pneumoniae* genes with important virulence functions, we plotted the fitness values of each clone across *in vitro* and *in vivo* conditions. This analysis identified sgRNA0370 targeting the gene *spv_0960* (*lafB*, a.k.a. *cpoA*), previously deemed as essential in Tn-seq experiments,[35] to be significantly underrepresented *in vivo* (Figure 1B; Table S1).

To validate the CRISPRi-seq screen, *lafB*-deleted and -complemented mutants were constructed (Figures S1E and S1F). Competition assays were conducted 7 days post influenza infection with wild-type (WT) *S. pneumoniae* paired with a *lafB* mutant or a *cps* mutant (avirulent control). *S. pneumoniae* lacking LafB were outcompeted by WT bacteria in lungs (Figure 1C). These results were confirmed in single-strain superinfection experiments as *lafB* mutant bacteria were significantly reduced in bacterial counts, compared with the WT or *lafB*-complemented strains (Figure 1D). Invasive disease, assessed by splenic dissemination, was likewise attenuated in animals infected with the *lafB* mutant (Figures S1G and S1H).

LafB is an intracellular membrane-associated protein involved in cell wall homeostasis

LafB (347 amino acids, 40 kDa)[36] is conserved among pneumococci (>96% amino acid identity in all sequenced pneumococci) (Figures S1J and S1K) and is implicated in the production of galactosyl-glucosyl-diacylglycerol, a glycolipid of unknown function (Figure 2A).[37,38] Incubation of recombinant LafB with α-monoglucosyldiacylglycerol (mGlc-DAG) and UDP-galactose followed by mass spectrometry, demonstrated the production of UDP (Figures S2A–S2D), establishing that LafB is a diglucosyl diacylglycerol synthase, as proposed previously.[39] Additionally, *lafB*-deficient pneumococci have a slightly reduced susceptibility to penicillins[37] but an increased susceptibility to daptomycin and acidic stress.[38,40] Prior immunoblot analysis found that LafB co-purifies with the membrane fraction.[37] However, while our structure prediction using RoseTTAFold[41] demonstrates the Rossmann-like domain of GT-B glycosyltransferases,[42] transmembrane domains were not detected (Figure 2B). Overlay of our predicted model of LafB to a related GT-B glycosyltransferase, *Mycobacterium tuberculosis* PimA (PDB: 2GEK),[43] showed good agreement, albeit with deviations in the active site cleft (Figure S1M).

To pinpoint LafB cellular localization, we constructed a functional GFP-LafB fusion (Figures S1I and S1L) and performed fluorescence microscopy. As shown in Figure 2C, GFP-LafB demonstrates membrane-associated localization. Split complementation luciferase assays for topology showed that both LafB termini reside in the cytoplasm (Figure 2D). The intracellular localization of LafB was further substantiated using a LafB-specific antibody binding assay (Figures S2F–S2H). These data support that LafB is an intracellular protein that is associated via hydrophobic and charge interactions with the cytoplasmic membrane.

To gain insight into *lafB* mutant virulence attenuation, we performed a synthetic lethal screen by introducing a genome-wide sgRNA library into the Δ*lafB* mutant background (Figure 2E). As shown in Figure 2F, the gene encoding the division protein DivIB[44] becomes essential in a *lafB* mutant, suggesting that galactosyl-glucosyl-diacylglycerol plays a role for efficient cell division. The gene *cozE* (a.k.a. *cozEa*) encoding a regulator of penicillin-binding protein Pbp1A[45] becomes less essential in the absence of *lafB* (Figure 2F). This genetic interaction may reflect prior findings that *cozE* mutants have deranged Pbp1A activity, causing cell lysis.[45] Since *lafB* mutants have reduced Pbp1A levels,[37] a double *lafB*/*cozE* knockdown alleviates the *cozE* single-mutant phenotype. Testing individual knockdowns of *divIB* and *cozE* validated the screen (Figure 2G).

Given that LafB uses the same lipid anchor as TacL to produce lipoteichoic acids (LTA),[46,47] we hypothesized that *lafB* deletion would accumulate the substrate for LTA (Figure 2A), resulting in an increased quantity of teichoic acids. Therefore, we quantified the phosphorylcholine levels in the *lafB* mutant using a specific antibody (TEPC-15) and flow cytometry. Indeed, the *lafB* mutant displayed a higher amount of phosphorylcholine on its cell surface than WT (Figures S2I and S2J). This observation suggests that LafB plays a crucial role in the homeostasis of teichoic acids.

Vaccination with LafB induces antigen-specific adaptive immune responses

To establish whether LafB is a protective antigen, we produced the *S. pneumoniae* D39V LafB protein in *E. coli* (Figure S2A). Recombinant LafB was formulated with alum as adjuvant for subcutaneous (s.c.) immunization or with the recombinant bacterial flagellin $FliC_{\Delta 174\text{-}400}$ as an adjuvant[48–50] for i.n. immunization. Flagellin has emerged as a safe and potent adjuvant by respiratory route against a variety of pathogens.[51] Immune responses specific for LafB were tested in mice on day 28 after a prime-boost vaccination (Figure 3A). A strong LafB-specific antibody response (IgG and IgM but no IgA) was observed for s.c.-vaccinated animals in serum and broncho-alveolar lavages, respectively (Figures 3B and S3A–S3D). In contrast, LafB-specific antibodies were weakly elicited in mice vaccinated via the i.n. route. When immune cells from lung, spleen, and mediastinal lymph nodes (MdLN) were stimulated *ex vivo* with LafB, cytokines associated with Th1 (IFN-γ), Th2 (IL-13), and Th17 (IL-17/IL-22) were produced in response, regardless of the vaccination route (Figures 3C, S3E, and S3F).

Intranasal vaccination offers broad protection across serotypes

Vaccinated animals were infected on day 28 with H3N2 influenza virus and superinfected on day 35 with serotype 2 strain D39V

(D) HiBiT assays showed that both N and C termini are localized inside the cytoplasm. Luminescence (relative light units, RLUs) is recorded with a microplate reader.
(E) CRISPRi-seq in wild-type (WT) D39V and *lafB* knockout mutant (Δ*lafB*) to identify the gene interaction network.
(F) Fitness cost of gene depletion between WT and Δ*lafB* mutant.
(G) Growth curve of WT and Δ*lafB* mutant with doxycycline-inducible CRISPRi targeting *cozE* and *divIB*. Strains were grown in C + Y medium with (10 ng/ml) or without (0 ng/ml) doxycycline, and the optical density at 595 nm was measured every 10 min. Average of 3 replicates is presented.

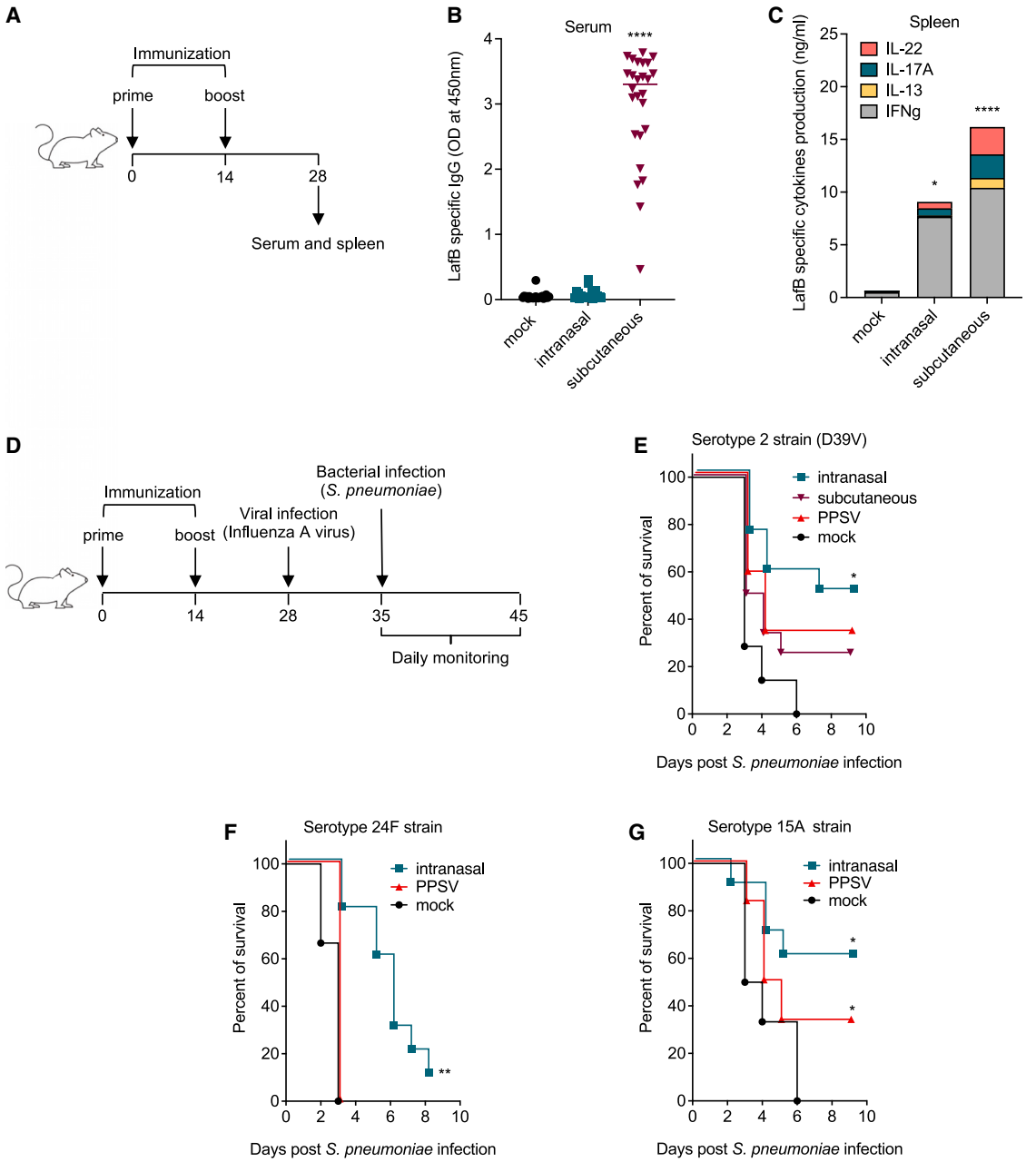

Figure 3. Intranasal vaccination with LafB protects mice against pneumococcal disease in a serotype-independent manner

(A) C57BL/6 mice were immunized on days 0 and 14 with LafB via intranasal (flagellin-adjuvanted) or subcutaneous (alum-adjuvanted) route, with a commercial PPSV vaccine, or were untreated (mock).

(B) LafB-specific antibody response. Sera were collected (22 mock, 26 intranasal, 26 subcutaneous), and levels of LafB-specific IgG were determined by ELISA. Plots represent medians and values for individual mice. Results are pooled from 3 experiments.

(C) Spleen cells (8 mice per group) were stimulated for 72 h with LafB, and cytokine levels were determined by ELISA. Results are expressed as median and are a pool of 2 experiments. Statistical significance (*$p < 0.05$, ****$p < 0.0001$) was assessed by one-way ANOVA Kruskal-Wallis test with Dunn's correction.

(D–G) (D) Vaccinated mice were infected with H3N2 influenza A virus on day 28 and were challenged on day 35 intranasally with *S. pneumoniae*. Survival with serotype 2 D39V strain (E, 5×10^4 CFU; 7 mock, 12 PPSV, 12 intranasal, 12 subcutaneous) is representative of 5 experiments. Results with serotype 24F (F, 10^3 CFU; 6 mock, 6 PPSV, 10 intranasal) are representative of 2 experiments, and results with serotype 15A strain (G, 5×10^4 CFU; 6 mock, 6 PPSV, 10 intranasal) are from one experiment. (E–G) Protection was assessed by monitoring survival. Statistical significance (*$p < 0.05$, ****$p < 0.0001$) was assessed by Mantel-Cox test.

CellPress
OPEN ACCESS

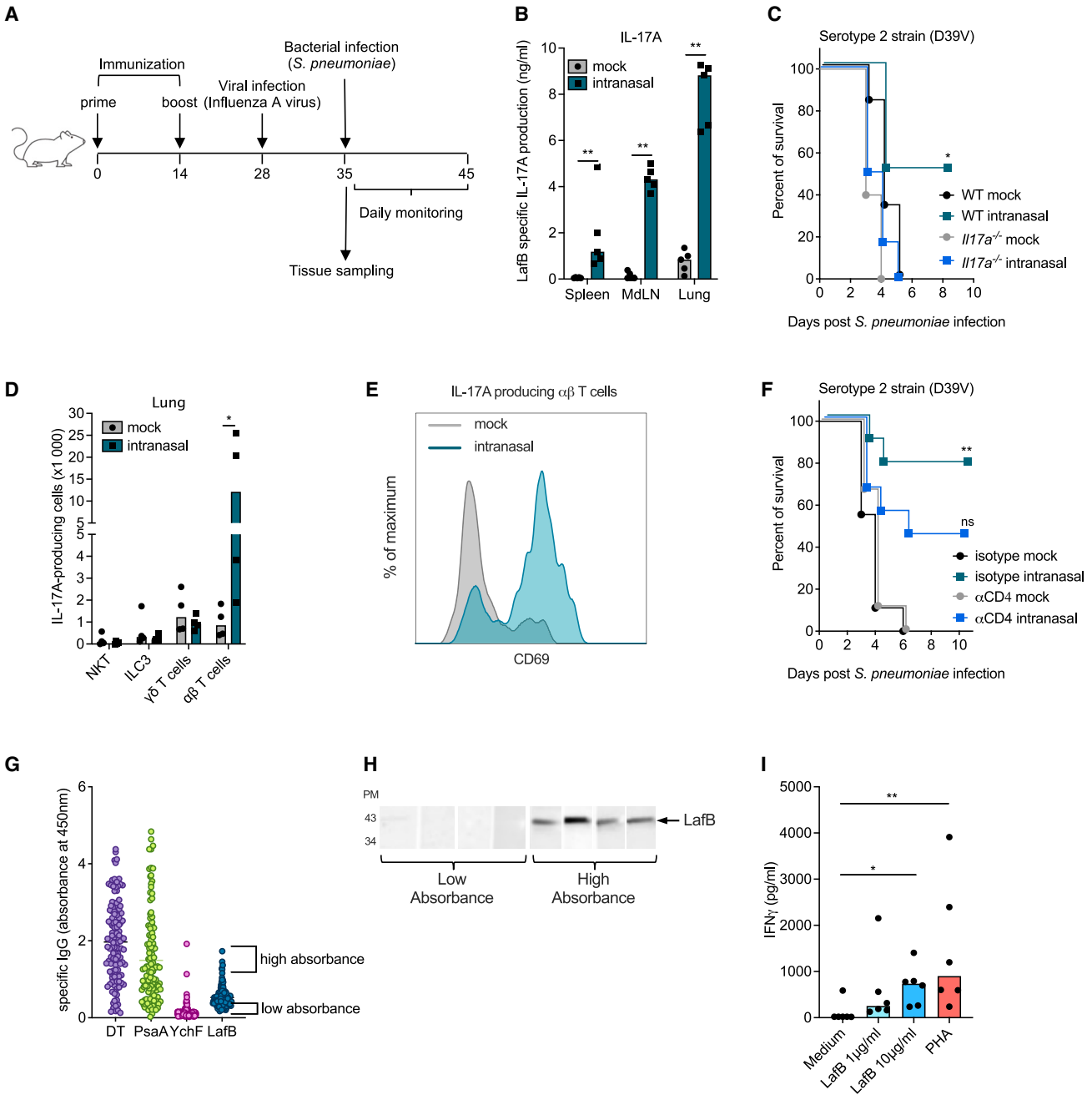

Figure 4. Th17 TRM-mediated protection in mice and LafB-specific immune responses in humans

(A) C57BL/6 (WT), *Rorc(t)-Gfp*^{TG}, or *Il17a*$^{-/-}$ mice were immunized on days 0 and 14 with flagellin-adjuvanted LafB by intranasal route or left unvaccinated (mock) and infected with H3N2 influenza A virus on day 28. On day 35, the immune responses of virus-infected animals in (B), (D), and (E) were analyzed, or the animals were superinfected with *S. pneumoniae* strain D39V (5×10^4 CFU) to monitor survival in (C) and (F).

(B) Spleen, MdLN, and lung cells from C57BL/6 animals (n = 5 per group) were collected and stimulated for 72 h with LafB antigen. IL-17A levels in supernatant were determined by ELISA. Plots represent medians and values for individual mice. Results are representative of 2 experiments. Statistical significance (**$p < 0.01$) was assessed by Mann-Whitney test.

(C) Vaccine protection is abolished in *Il17a*$^{-/-}$ mice. Results are from one experiment with 6 animals per group. Statistical significance (*$p < 0.05$) was assessed by Mantel-Cox test.

(D and E) ROR γt- and IL-17A-producing lung cells in *Rorc(t)-Gfp*^{TG} animals. Results are representative of 2 experiments with 4 mice per group. (D) Analysis of natural killer T (NKT) cells, group 3 innate lymphoid cells (ILC3), TCRγδ T cells, and conventional αβ T lymphocytes. Plots represent medians and values for individual mice. Statistical significance (*$p < 0.01$) was assessed by Mann-Whitney test. (E) Expression of CD69 marker on lung CD4$^+$ Th17 cells.

(F) Protection requires CD4$^+$ T cells. To this end, mice (n = 9 per group) were treated intraperitoneally on day 34 with CD4-specific depleting antibodies or control isotype, infected on day 35 with D39V, and protection was assessed. Results are representative of 2 experiments. Statistical significance (**$p < 0.01$) was assessed by Mantel-Cox test.

(legend continued on next page)

(Figure 3D). All mice receiving mock immunization succumbed to disease after infection. Forty percent of mice vaccinated with PPSV, which includes the CPS from serotype 2, were protected against pneumococcal challenge (Figure 3E). Mice vaccinated via the i.n. route with flagellin-adjuvanted LafB outperformed both s.c.- and PPSV-vaccinated animals, with 60% mouse survival. Protection was associated with reduced weight loss during the first day following the D39V infection (Figure S4A). Moreover, surviving mice were consistently gaining weight from day 3 (Figure S4B). Mice immunized i.n. with vaccines containing LafB standalone or flagellin-adjuvanted ovalbumin were not protected (Figures S3H and S3I).

Immunoblotting showed that serum of animals vaccinated with flagellin-adjuvanted LafB recognized strains representing serotypes 1, 3, 4, 5, 9V, 11A, 15A, 19F, 23A, 23F, 24F, and 35B, corroborating the conservation of LafB (Figure S2E). Since the introduction of the CPS-based vaccines, serotypes 15A and 24F are becoming prevalent,[8,52,53] which are not included in PPSV (that does contain 15B, which is cross-reactive to 15A).[54] Flagellin-adjuvanted LafB vaccination significantly protected mice against infection with the 15A and 24F strains, in contrast to mice vaccinated with PPSV, which only offered slight protection against serotype 15A (Figures 3F and 3G). Protection was supported by weight analysis (Figures S4C–S4F). LafB-vaccinated mice completely cleared pneumococcal bacteria (Figure S4G), supporting a role for LafB as a universal vaccine antigen to confer sterilizing protection.

Protection against pneumococcal superinfection is mediated by Th17 immunity

Th17 CD4$^+$ T lymphocytes that are functionally characterized by the expression of the retinoid orphan receptor γ t (RORγt) and the production of IL-17A, are essential for mucosal protection against pneumococcal infection.[55–58] To study the mechanisms of protection, immune responses were monitored starting from day 35, a time when viral infection impairs the innate and cell-mediated immunity[59–63] (Figure 4A). Cells isolated from spleen, MdLN, or lung from vaccinated animals secreted IL-17A after *ex vivo* stimulation with LafB (Figure 4B), indicating that influenza infection did not disturb the capacity of the vaccine to stimulate IL-17A. Moreover, vaccination did not alter viral replication or the virus-induced proinflammatory response, when compared with mock or s.c. immunization, as measured by the viral RNA and markers for inflammation (Figures S4H and S4I). In contrast to WT animals, *Il17a*-deficient mice were not protected against superinfection after i.n. vaccination (Figure 4C). Notably, the lung viral RNA quantities were unchanged in *Il17a*-deficient mice, and the infection remained sublethal (Figures S4J and S4K). Together, these data show that IL-17A is a major effector of immunoprotective response induced by LafB i.n. vaccination.

The main cells producing RORγt and IL-17A after i.n. vaccination and influenza virus infection were conventional CD4$^+$ T lymphocytes expressing TCR$\alpha\beta$, i.e., Th17 lymphocytes (Figures 4D and 4E). Other innate lymphocytes, such as natural killer T cells, group 3 innate lymphoid cells, or TCR$\gamma\delta$ T cells, were moderately affected. Th17 lymphocytes were associated with increased surface expression of CD69, a marker specific of tissue-resident memory (TRM) T lymphocytes in lungs.[64] Depletion of CD4$^+$ T lymphocytes also reduced protection of the LafB vaccine against pneumococcal disease (Figure 4F). Thus, i.n. LafB vaccination induced protection dependent on lung Th17 lymphocytes with TRM features.

Healthy human individuals develop LafB-specific immunity

To examine whether LafB might be a suitable vaccine and antigenic in humans, we screened plasma from >100 healthy donors for antigen-specific antibodies. Diphtheria toxoid was used as a positive control. The pneumococcal proteins PsaA and YchF were used as supplementary antigens. As shown in Figure 4G, individuals were all immunoreactive to diphtheria toxoid. LafB-specific antibody responses were rather low. However, 10% of individuals demonstrated a stronger LafB antibody response. The responses for PsaA and YchF were also heterogeneous and variable. Using immunoblotting, we found that immunoreactivity was associated to LafB detection (Figure 4H). Finally, peripheral blood mononuclear cells from healthy donors were stimulated with recombinant LafB or incubated with T cell stimulant phytohemagglutinin (Figure 4I). LafB significantly stimulated IFN-γ secretion, compared with controls. Together, these data indicate that LafB is antigenic in humans.

DISCUSSION

The principal contribution of this work is the identification of a conserved intracellular membrane-associated pneumococcal antigen as a vaccine candidate effective in protection, even following influenza virus infection. The unbiased approach of antigen screening by CRISPRi in the context of superinfection defined that the protein LafB plays an essential role in pneumococcal virulence. LafB indirectly controls the levels of teichoic acids by using the lipid anchor Glc-DAG to synthesize GalGlc-DAG, similarly to TacL in the production of LTA[46,47] (Figure S2). Indeed, LafB is important for proper cell envelope homeostasis, offering an explanation for why LafB is conserved and important for virulence. Despite its intracellular localization, LafB triggers vigorous antibody- and T cell-mediated immunity. This paradigm for antigen selection may open avenues for the discovery of virulence-associated antigens heretofore overlooked by classical approaches. In contrast to surface determinants, LafB may be exposed outside of bacteria upon the production of extracellular vesicles,[65] lysis, or autolysis. Indeed, during colonization, pneumococci establish biofilms that consist of a matrix of lysed bacteria.[66] A subset of healthy individuals have LafB-specific

(G) Plasma samples from healthy donors (n = 127) were analyzed by ELISA for reactivity specific to the following antigens: diphtheria toxoid (DT) and the pneumococcal proteins LafB, PsaA, and YchF. Plots represent medians and values for individual donors.
(H) Plasma samples (n = 4 per group) with low and high absorbance at 450 nm in ELISA were analyzed by immunoblotting. LafB was separated by SDS-PAGE and transferred to a membrane before probing with plasma.
(I) Peripheral blood mononuclear cells from healthy donors (n = 6) were stimulated for 5 days with LafB or phytohemagglutinin (PHA) or were untreated. Secretion of IFN-γ was determined by ELISA. Statistical significance (*$p < 0.05$, ***$p < 0.001$) was assessed by one-way ANOVA Kruskal-Wallis test with Dunn's correction.

CellPress
OPEN ACCESS

IgG in their serum, indicating that LafB is also antigenic in humans. It should be noted that LafB is highly conserved in pneumococci (Figure S1), and to a lesser extent in members of the *mitis* groups, meaning that LafB-specific antibodies do not strictly indicate previous pneumococcal carriage or infection. Unraveling the immune circuits underlying the respiratory protective response is an important question for future research. In addition, it would be interesting to test the efficacy of i.n. vaccination against primary pneumonia caused by pneumococcus.

Multiple lines of evidence show that Th17 lymphocytes are instrumental for protecting the respiratory mucosa against pneumococcal infection.[55–58,67,68] Moreover, preceding influenza virus infection may blunt IL-17 production by $\gamma\delta$ T cells in response to *S. pneumoniae*.[69] Cross-protection against pneumococcal diseases after recovery from a primary infection is mediated by memory Th17 cells, but the antigenic determinants remained to be defined.[58] Interestingly, memory Th17 responses elicited by pneumococcal infection can overcome viral-driven Th17 inhibition and provide cross-protection against different serotypes during co-infection with influenza virus. Thus, a vaccine that drives Th17 responses could mitigate disease caused by co-infection.[70] LafB may constitute such a prototypic cross-protective antigen. Recent studies highlighted how lung Th17 cells differentiate into TRM that persist in tissue, promote long-term protection against pathogens,[57,64] and are less prone to collapse in the context of immunosuppression.[57] Stimulation of lung Th17 lymphocytes and TRM may explain the inferior protective capacity of systemic route of immunization. Similar observations were made for COVID-19 vaccination in which antibody levels do not correlate with better disease outcome, particularly in older individuals.[71] A next generation of vaccines could incorporate CPS conjugated to LafB for intramuscular priming, followed by an i.n. boost with adjuvanted LafB. This vaccination regimen is poised to induce (1) high-affinity opsonizing circulating antibodies against CPS and (2) lung-resident memory Th17 cells. These two arms of adaptive immunity might operate synergistically in systemic and mucosal compartments, contributing to reduced carriage and immunoprotection. The use of mucosal adjuvants to potentiate lung protective immunity is an expanding field of research that will lay the foundation of a new generation of vaccines against respiratory pathogens.[57,72,73]

STAR★METHODS

Detailed methods are provided in the online version of this paper and include the following:

- KEY RESOURCES TABLE
- RESOURCE AVAILABILITY
  - Lead contact
  - Materials availability
  - Data and code availability
- EXPERIMENTAL MODELS AND SUBJECT DETAILS
  - Bacterial strains and culture conditions
  - Mouse models
  - Murine superinfection assays
  - Human samples
- METHODS DETAILS
  - Phase contrast and fluorescence microscopy
  - Split-luciferase HiBiT-tag detection system assay
  - Bacterial genomic DNA extraction and CRISPRi-seq
  - LafB synthetic lethal screening by CRISPRi-seq
  - Mice vaccination
  - Antigen-specific immune responses
  - Flow cytometry analysis
  - Analysis of plasma and PBMC from healthy individuals
  - Rabbit LafB antiserum
  - Western blot and immunoblot
  - Doxycycline stock
  - Purification of LafB and YchF protein from *E. coli*
  - Biochemical characterization of the LafB glycosylation activity
  - Bacterial colonization
  - Viral RNA quantification
  - Proinflammatory gene expression
  - Strain construction
  - Antisera production in rabbit used for western blotting
- QUANTIFICATION AND STATISTICAL ANALYSIS
- ADDITIONAL RESOURCES
- DATA AND MATERIALS AVAILABILITY

SUPPLEMENTAL INFORMATION

Supplemental information can be found online at https://doi.org/10.1016/j.chom.2024.02.002.

ACKNOWLEDGMENTS

We thank Mara Baldry and Charlotte Costa for assistance with animal experiments, Frédéric Wallet for clinical isolates, Loic Coutte for *Il17a*$^{-/-}$ mice, Delphine Cayet for ELISA, Guillaume Lefebvre and Julie Démaret for discussions, Cyrille Grandjean for PsaA, and Jingwei Xu for RoseTTAFold predictions. We thank UNIL's Metabolomics and Genomics Technologies Facility, UAR2014-US41-PLBS, Bioimaging Center Lille, Flow Cytometry Core Facility, and the PLETHA animal facility. This work was supported by an ERC consolidator grant (771534) and Swiss National Science Foundation grants (310030_192517, 310030_200792, 51NF40_180541, and IZSEZ0_213879) to J.-W.V.; Inserm, Institut Pasteur de Lille, Université de Lille, and the Structure Fédérative de Recherche grant PneumoVac to L.V.M.; the project FAIR, which received funding from the European Union's Horizon 2020 research and innovation programme under grant agreement no. 847786 to J.-C.S.; a National Nature Science Foundation of China grant (82270012), the Science and Technology Project of Shenzhen (JCYJ20220818095602006), and the Shenzhen University 2035 Program for Excellent Research (86901-00000216) to X.L.

AUTHOR CONTRIBUTIONS

Experimentation, X.L., L.V.M., D.S., L.M., V.A.D.d.S., J.D., F.P.B., M.T., and J.O.; study design and analysis, X.L., L.V.M., L.M., V.d.B., S.G., and J.-W.V.; writing – original draft, X.L., L.V.M., J.-C.S., and J.-W.V.; writing – review & editing, X.L., V.N., J.-C.S., and J.-W.V.

DECLARATION OF INTERESTS

X.L., L.V.M., F.P.B., J.-C.S., and J.-W.V. have filed patent application WO 2023/006825 on aspects of this work. J.-C.S. is the inventor of patent WO2009156405, describing recombinant flagellin as an adjuvant.

Received: January 24, 2023
Revised: December 6, 2023
Accepted: February 5, 2024
Published: February 27, 2024

REFERENCES

1. McCullers, J.A. (2014). The co-pathogenesis of influenza viruses with bacteria in the lung. Nat. Rev. Microbiol. *12*, 252–262.
2. Chertow, D.S., and Memoli, M.J. (2013). Bacterial coinfection in influenza: a grand rounds review. JAMA *309*, 275–282.
3. Madhi, S.A., Schoub, B., and Klugman, K.P. (2008). Interaction between influenza virus and *Streptococcus pneumoniae* in severe pneumonia. Expert Rev. Respir. Med. *2*, 663–672.
4. Lindsay, M.I., Herrmann, E.C., Morrow, G.W., and Brown, A.L. (1970). Hong Kong influenza: clinical, microbiologic, and pathologic features in 127 cases. JAMA *214*, 1825–1832.
5. Scott, N.R., Mann, B., Tuomanen, E.I., and Orihuela, C.J. (2021). Multi-Valent Protein Hybrid Pneumococcal Vaccines: A Strategy for the Next Generation of Vaccines. Vaccines *9*, 209.
6. Pletz, M.W., Maus, U., Krug, N., Welte, T., and Lode, H. (2008). Pneumococcal vaccines: mechanism of action, impact on epidemiology and adaption of the species. Int. J. Antimicrob. Agents *32*, 199–206.
7. Davies, L.R.L., Cizmeci, D., Guo, W., Luedemann, C., Alexander-Parrish, R., Grant, L., Isturiz, R., Theilacker, C., Jodar, L., Gessner, B.D., et al. (2022). Polysaccharide and conjugate vaccines to *Streptococcus pneumoniae* generate distinct humoral responses. Sci. Transl. Med. *14*, eabm4065.
8. Løchen, A., Croucher, N.J., and Anderson, R.M. (2020). Divergent serotype replacement trends and increasing diversity in pneumococcal disease in high income settings reduce the benefit of expanding vaccine valency. Sci. Rep. *10*, 18977.
9. Wang, L.M., Cravo Oliveira Hashiguchi, T., and Cecchini, M. (2021). Impact of vaccination on carriage of and infection by antibiotic-resistant bacteria: a systematic review and meta-analysis. Clin. Exp. Vaccin. Res. *10*, 81–92.
10. Ganaie, F., Saad, J.S., McGee, L., van Tonder, A.J., Bentley, S.D., Lo, S.W., Gladstone, R.A., Turner, P., Keenan, J.D., Breiman, R.F., et al. (2020). A New Pneumococcal Capsule Type, 10D, is the 100th Serotype and Has a Large cps Fragment from an Oral Streptococcus. mBio *11*, e00937-20.
11. Scelfo, C., Menzella, F., Fontana, M., Ghidoni, G., Galeone, C., and Facciolongo, N.C. (2021). Pneumonia and Invasive Pneumococcal Diseases: The Role of Pneumococcal Conjugate Vaccine in the Era of Multi-Drug Resistance. Vaccines *9*, 420.
12. Weinberger, D.M., Malley, R., and Lipsitch, M. (2011). Serotype replacement in disease after pneumococcal vaccination. Lancet *378*, 1962–1973.
13. Essink, B., Sabharwal, C., Cannon, K., Frenck, R., Lal, H., Xu, X., Sundaraiyer, V., Peng, Y., Moyer, L., Pride, M.W., et al. (2022). Pivotal Phase 3 Randomized Clinical Trial of the Safety, Tolerability, and Immunogenicity of 20-Valent Pneumococcal Conjugate Vaccine in Adults Aged $\geq$18 Years. Clin. Infect. Dis. *75*, 390–398.
14. Platt, H.L., Cardona, J.F., Haranaka, M., Schwartz, H.I., Narejos Perez, S., Dowell, A., Chang, C.J., Dagan, R., Tamms, G.M., Sterling, T., et al. (2022). A phase 3 trial of safety, tolerability, and immunogenicity of V114, 15-valent pneumococcal conjugate vaccine, compared with 13-valent pneumococcal conjugate vaccine in adults 50 years of age and older (PNEU-AGE). Vaccine *40*, 162–172.
15. Metzger, D.W., Furuya, Y., Salmon, S.L., Roberts, S., and Sun, K. (2015). Limited Efficacy of Antibacterial Vaccination Against Secondary Serotype 3 Pneumococcal Pneumonia Following Influenza Infection. J. Infect. Dis. *212*, 445–452.
16. Jirru, E., Lee, S., Harris, R., Yang, J., Cho, S.J., and Stout-Delgado, H. (2020). Impact of Influenza on Pneumococcal Vaccine Effectiveness during *Streptococcus pneumoniae* Infection in Aged Murine Lung. Vaccines *8*, 298.
17. Smith, A.M., and Huber, V.C. (2018). The Unexpected Impact of Vaccines on Secondary Bacterial Infections Following Influenza. Viral Immunol. *31*, 159–173.
18. Carniel, B.F., Marcon, F., Rylance, J., German, E.L., Zaidi, S., Reiné, J., Negera, E., Nikolaou, E., Pojar, S., Solórzano, C., et al. (2021). Pneumococcal colonization impairs mucosal immune responses to live attenuated influenza vaccine. JCI Insight *6*, e141088.
19. Giefing, C., Meinke, A.L., Hanner, M., Henics, T., Bui, M.D., Gelbmann, D., Lundberg, U., Senn, B.M., Schunn, M., Habel, A., et al. (2008). Discovery of a novel class of highly conserved vaccine antigens using genomic scale antigenic fingerprinting of pneumococcus with human antibodies. J. Exp. Med. *205*, 117–131.
20. Gierahn, T., and Malley, R. (2011). Vaccines and compositions against Streptococcus pneumoniae. US patent US20110020386A1. filed June 29, 2010, and published January 27, 2011.
21. Lu, Y.J., Oliver, E., Zhang, F., Pope, C., Finn, A., and Malley, R. (2018). Screening for Th17-Dependent Pneumococcal Vaccine Antigens: Comparison of Murine and Human Cellular Immune Responses. Infect. Immun. *86*, e00490-18.
22. Nabors, G.S., Braun, P.A., Herrmann, D.J., Heise, M.L., Pyle, D.J., Gravenstein, S., Schilling, M., Ferguson, L.M., Hollingshead, S.K., Briles, D.E., et al. (2000). Immunization of healthy adults with a single recombinant pneumococcal surface protein A (PspA) variant stimulates broadly cross-reactive antibodies to heterologous PspA molecules. Vaccine *18*, 1743–1754.
23. Schmid, P., Selak, S., Keller, M., Luhan, B., Magyarics, Z., Seidel, S., Schlick, P., Reinisch, C., Lingnau, K., Nagy, E., et al. (2011). Th17/Th1 biased immunity to the pneumococcal proteins PcsB, StkP and PsaA in adults of different age. Vaccine *29*, 3982–3989.
24. Voß, F., Kohler, T.P., Meyer, T., Abdullah, M.R., van Opzeeland, F.J., Saleh, M., Michalik, S., van Selm, S., Schmidt, F., de Jonge, M.I., et al. (2018). Intranasal Vaccination With Lipoproteins Confers Protection Against Pneumococcal Colonisation. Front. Immunol. *9*, 2405.
25. Nakahashi-Ouchida, R., Uchida, Y., Yuki, Y., Katakai, Y., Yamanoue, T., Ogawa, H., Munesue, Y., Nakano, N., Hanari, K., Miyazaki, T., et al. (2021). A nanogel-based trivalent PspA nasal vaccine protects macaques from intratracheal challenge with pneumococci. Vaccine *39*, 3353–3364.
26. van Beek, L.F., Langereis, J.D., van den Berg van Saparoea, H.B., Gillard, J., Jong, W.S.P., van Opzeeland, F.J., Mesman, R., van Niftrik, L., Joosten, I., Diavatopoulos, D.A., et al. (2021). Intranasal vaccination with protein bodies elicit strong protection against *Streptococcus pneumoniae* colonization. Vaccine *39*, 6920–6929.
27. Croucher, N.J., Løchen, A., and Bentley, S.D. (2018). Pneumococcal Vaccines: Host Interactions, Population Dynamics, and Design Principles. Annu. Rev. Microbiol. *72*, 521–549.
28. Slager, J., Aprianto, R., and Veening, J.W. (2018). Deep genome annotation of the opportunistic human pathogen *Streptococcus pneumoniae* D39. Nucleic Acids Res. *46*, 9971–9989.
29. Croucher, N.J., Campo, J.J., Le, T.Q., Liang, X., Bentley, S.D., Hanage, W.P., and Lipsitch, M. (2017). Diverse evolutionary patterns of pneumococcal antigens identified by pangenome-wide immunological screening. Proc. Natl. Acad. Sci. USA *114*, E357–E366.
30. Georgieva, M., Kagedan, L., Lu, Y.J., Thompson, C.M., and Lipsitch, M. (2018). Antigenic Variation in *Streptococcus pneumoniae* PspC Promotes Immune Escape in the Presence of Variant-Specific Immunity. mBio *9*, e00264-18.
31. Rowe, H.M., Karlsson, E., Echlin, H., Chang, T.C., Wang, L., van Opijnen, T., Pounds, S.B., Schultz-Cherry, S., and Rosch, J.W. (2019). Bacterial Factors Required for Transmission of *Streptococcus pneumoniae* in Mammalian Hosts. Cell Host Microbe *25*, 884–891.e6.
32. Zangari, T., Zafar, M.A., Lees, J.A., Abruzzo, A.R., Bee, G.C.W., and Weiser, J.N. (2021). Pneumococcal capsule blocks protection by immunization with conserved surface proteins. npj Vaccines *6*, 155.
33. de Bakker, V., Liu, X., Bravo, A.M., and Veening, J.W. (2022). CRISPRi-seq for genome-wide fitness quantification in bacteria. Nat. Protoc. *17*, 252–281.

34. Liu, X., Kimmey, J.M., Matarazzo, L., de Bakker, V., Van Maele, L., Sirard, J.C., Nizet, V., and Veening, J.W. (2021). Exploration of Bacterial Bottlenecks and *Streptococcus pneumoniae* Pathogenesis by CRISPRi-Seq. Cell Host Microbe *29*, 107–120.e6.

35. van Opijnen, T., and Camilli, A. (2012). A fine scale phenotype-genotype virulence map of a bacterial pathogen. Genome Res. *22*, 2541–2551.

36. Webb, A.J., Karatsa-Dodgson, M., and Gründling, A. (2009). Two-enzyme systems for glycolipid and polyglycerolphosphate lipoteichoic acid synthesis in *Listeria monocytogenes*. Mol. Microbiol. *74*, 299–314.

37. Grebe, T., Paik, J., and Hakenbeck, R. (1997). A novel resistance mechanism against beta-lactams in *Streptococcus pneumoniae* involves CpoA, a putative glycosyltransferase. J. Bacteriol. *179*, 3342–3349.

38. Meiers, M., Volz, C., Eisel, J., Maurer, P., Henrich, B., and Hakenbeck, R. (2014). Altered lipid composition in *Streptococcus pneumoniae cpoA* mutants. BMC Microbiol. *14*, 12.

39. Edman, M., Berg, S., Storm, P., Wikström, M., Vikström, S., Ohman, A., and Wieslander, A. (2003). Structural features of glycosyltransferases synthesizing major bilayer and nonbilayer-prone membrane lipids in *Acholeplasma laidlawii* and *Streptococcus pneumoniae*. J. Biol. Chem. *278*, 8420–8428.

40. Rosconi, F., Rudmann, E., Li, J., Surujon, D., Anthony, J., Frank, M., Jones, D.S., Rock, C., Rosch, J.W., Johnston, C.D., et al. (2022). A bacterial pan-genome makes gene essentiality strain-dependent and evolvable. Nat. Microbiol. *7*, 1580–1592.

41. Baek, M., DiMaio, F., Anishchenko, I., Dauparas, J., Ovchinnikov, S., Lee, G.R., Wang, J., Cong, Q., Kinch, L.N., Schaeffer, R.D., et al. (2021). Accurate prediction of protein structures and interactions using a three-track neural network. Science *373*, 871–876.

42. Chang, A., Singh, S., Phillips, G.N., and Thorson, J.S. (2011). Glycosyltransferase structural biology and its role in the design of catalysts for glycosylation. Curr. Opin. Biotechnol. *22*, 800–808.

43. Guerin, M.E., Kordulakova, J., Schaeffer, F., Svetlikova, Z., Buschiazzo, A., Giganti, D., Gicquel, B., Mikusova, K., Jackson, M., and Alzari, P.M. (2007). Molecular Recognition and Interfacial Catalysis by the Essential Phosphatidylinositol Mannosyltransferase PimA from Mycobacteria. J. Biol. Chem. *282*, 20705–20714.

44. Le Gouëllec, A., Roux, L., Fadda, D., Massidda, O., Vernet, T., and Zapun, A. (2008). Roles of Pneumococcal DivIB in Cell Division. J. Bacteriol. *190*, 4501–4511.

45. Fenton, A.K., El Mortaji, L., Lau, D.T.C., Rudner, D.Z., and Bernhardt, T.G. (2016). CozE is a member of the MreCD complex that directs cell elongation in *Streptococcus pneumoniae*. Nat. Microbiol. *2*, 16237.

46. Flores-Kim, J., Dobihal, G.S., Fenton, A., Rudner, D.Z., and Bernhardt, T.G. (2019). A switch in surface polymer biogenesis triggers growth-phase-dependent and antibiotic-induced bacteriolysis. eLife *8*, e44912.

47. Heß, N., Waldow, F., Kohler, T.P., Rohde, M., Kreikemeyer, B., Gómez-Mejia, A., Hain, T., Schwudke, D., Vollmer, W., Hammerschmidt, S., et al. (2017). Lipoteichoic acid deficiency permits normal growth but impairs virulence of *Streptococcus pneumoniae*. Nat. Commun. *8*, 2093.

48. Biedma, M.E., Cayet, D., Tabareau, J., Rossi, A.H., Ivičak-Kocjan, K., Moreno, G., Errea, A., Soulard, D., Parisi, G., Jerala, R., et al. (2019). Recombinant flagellins with deletions in domains D1, D2, and D3: Characterization as novel immunoadjuvants. Vaccine *37*, 652–663.

49. Van Maele, L., Fougeron, D., Janot, L., Didierlaurent, A., Cayet, D., Tabareau, J., Rumbo, M., Corvo-Chamaillard, S., Boulenouar, S., Jeffs, S., et al. (2014). Airway structural cells regulate TLR5-mediated mucosal adjuvant activity. Mucosal Immunol. *7*, 489–500.

50. Nempont, C., Cayet, D., Rumbo, M., Bompard, C., Villeret, V., and Sirard, J.C. (2008). Deletion of Flagellin's Hypervariable Region Abrogates Antibody-Mediated Neutralization and Systemic Activation of TLR5-Dependent Immunity. J. Immunol. *181*, 2036–2043.

51. Vijayan, A., Rumbo, M., Carnoy, C., and Sirard, J.C. (2018). Compartmentalized Antimicrobial Defenses in Response to Flagellin. Trends Microbiol. *26*, 423–435.

52. Nakano, S., Fujisawa, T., Ito, Y., Chang, B., Matsumura, Y., Yamamoto, M., Suga, S., Ohnishi, M., and Nagao, M. (2019). Whole-Genome Sequencing Analysis of Multidrug-Resistant Serotype 15A *Streptococcus pneumoniae* in Japan and the Emergence of a Highly Resistant Serotype 15A-ST9084 Clone. Antimicrob. Agents Chemother. *63*, e02579-18.

53. Lo, S.W., Mellor, K., Cohen, R., Alonso, A.R., Belman, S., Kumar, N., Hawkins, P.A., Gladstone, R.A., von Gottberg, A., Veeraraghavan, B., et al. (2022). Emergence of a multidrug-resistant and virulent *Streptococcus pneumoniae* lineage mediates serotype replacement after PCV13: an international whole-genome sequencing study. Lancet Microbe *3*, e735–e743.

54. Hao, L., Kuttel, M.M., Ravenscroft, N., Thompson, A., Prasad, A.K., Gangolli, S., Tan, C., Cooper, D., Watson, W., Liberator, P., et al. (2022). *Streptococcus pneumoniae* serotype 15B polysaccharide conjugate elicits a cross-functional immune response against serotype 15C but not 15A. Vaccine *40*, 4872–4880.

55. Zhang, Z., Clarke, T.B., and Weiser, J.N. (2009). Cellular effectors mediating Th17-dependent clearance of pneumococcal colonization in mice. J. Clin. Invest. *119*, 1899–1909.

56. Trzciński, K., Thompson, C.M., Srivastava, A., Basset, A., Malley, R., and Lipsitch, M. (2008). Protection against Nasopharyngeal Colonization by *Streptococcus pneumoniae* Is Mediated by Antigen-Specific CD4+ T Cells. Infect. Immun. *76*, 2678–2684.

57. Shenoy, A.T., Wasserman, G.A., Arafa, E.I., Wooten, A.K., Smith, N.M.S., Martin, I.M.C., Jones, M.R., Quinton, L.J., and Mizgerd, J.P. (2020). Lung CD4+ resident memory T cells remodel epithelial responses to accelerate neutrophil recruitment during pneumonia. Mucosal Immunol. *13*, 334–343.

58. Wang, Y., Jiang, B., Guo, Y., Li, W., Tian, Y., Sonnenberg, G.F., Weiser, J.N., Ni, X., and Shen, H. (2017). Cross-protective mucosal immunity mediated by memory Th17 cells against *Streptococcus pneumoniae* lung infection. Mucosal Immunol. *10*, 250–259.

59. Barthelemy, A., Ivanov, S., Fontaine, J., Soulard, D., Bouabe, H., Paget, C., Faveeuw, C., and Trottein, F. (2017). Influenza A virus-induced release of interleukin-10 inhibits the anti-microbial activities of invariant natural killer T cells during invasive pneumococcal superinfection. Mucosal Immunol. *10*, 460–469.

60. Ivanov, S., Fontaine, J., Paget, C., Macho Fernandez, E., Van Maele, L., Renneson, J., Maillet, I., Wolf, N.M., Rial, A., Léger, H., et al. (2012). Key role for respiratory CD103(+) dendritic cells, IFN-γ, and IL-17 in protection against *Streptococcus pneumoniae* infection in response to α-galactosylceramide. J. Infect. Dis. *206*, 723–734.

61. Ivanov, S., Renneson, J., Fontaine, J., Barthelemy, A., Paget, C., Fernandez, E.M., Blanc, F., De Trez, C., Van Maele, L., Dumoutier, L., et al. (2013). Interleukin-22 reduces lung inflammation during influenza A virus infection and protects against secondary bacterial infection. J. Virol. *87*, 6911–6924.

62. Zangari, T., Ortigoza, M.B., Lokken-Toyli, K.L., and Weiser, J.N. (2021). Type I Interferon Signaling Is a Common Factor Driving *Streptococcus pneumoniae* and Influenza A Virus Shedding and Transmission. mBio *12*, e03589-20.

63. Sender, V., Hentrich, K., Pathak, A., Tan Qian Ler, A., Embaie, B.T., Lundström, S.L., Gaetani, M., Bergstrand, J., Nakamoto, R., Sham, L.T., et al. (2020). Capillary leakage provides nutrients and antioxidants for rapid pneumococcal proliferation in influenza-infected lower airways. Proc. Natl. Acad. Sci. USA *117*, 31386–31397.

64. Amezcua Vesely, M.C., Pallis, P., Bielecki, P., Low, J.S., Zhao, J., Harman, C.C.D., Kroehling, L., Jackson, R., Bailis, W., Licona-Limón, P., et al. (2019). Effector TH17 Cells Give Rise to Long-Lived TRM Cells that Are Essential for an Immediate Response against Bacterial Infection. Cell *178*, 1176–1188.e15.

65. Yerneni, S.S., Werner, S., Azambuja, J.H., Ludwig, N., Eutsey, R., Aggarwal, S.D., Lucas, P.C., Bailey, N., Whiteside, T.L., Campbell, P.G., et al. (2021). Pneumococcal Extracellular Vesicles Modulate Host Immunity. mBio *12*, e0165721.

66. Chao, Y., Marks, L.R., Pettigrew, M.M., and Hakansson, A.P. (2014). *Streptococcus pneumoniae* biofilm formation and dispersion during colonization and disease. Front. Cell. Infect. Microbiol. *4*, 194.

67. Kuipers, K., Jong, W.S.P., van der Gaast-de Jongh, C.E., Houben, D., van Opzeeland, F., Simonetti, E., van Selm, S., de Groot, R., Koenders, M.I., Azarian, T., et al. (2017). Th17-Mediated Cross Protection against Pneumococcal Carriage by Vaccination with a Variable Antigen. Infect. Immun. *85*, e00281-17.

68. Moffitt, K.L., Gierahn, T.M., Lu, Y.J., Gouveia, P., Alderson, M., Flechtner, J.B., Higgins, D.E., and Malley, R. (2011). TH17-based vaccine design for prevention of *Streptococcus pneumoniae* colonization. Cell Host Microbe *9*, 158–165.

69. Li, W., Moltedo, B., and Moran, T.M. (2012). Type I interferon induction during influenza virus infection increases susceptibility to secondary *Streptococcus pneumoniae* infection by negative regulation of γδ T cells. J. Virol. *86*, 12304–12312.

70. Li, Y., Yang, Y., Chen, D., Wang, Y., Zhang, X., Li, W., Chen, S., Wong, S.M., Shen, M., Akerley, B.J., et al. (2023). Memory Th17 cell-mediated protection against lethal secondary pneumococcal pneumonia following influenza infection. mBio *0*, e00519-23.

71. Rydyznski Moderbacher, C., Ramirez, S.I., Dan, J.M., Grifoni, A., Hastie, K.M., Weiskopf, D., Belanger, S., Abbott, R.K., Kim, C., Choi, J., et al. (2020). Antigen-Specific Adaptive Immunity to SARS-CoV-2 in Acute COVID-19 and Associations with Age and Disease Severity. Cell *183*, 996–1012.e19.

72. Marinaik, C.B., Kingstad-Bakke, B., Lee, W., Hatta, M., Sonsalla, M., Larsen, A., Neldner, B., Gasper, D.J., Kedl, R.M., Kawaoka, Y., et al. (2020). Programming Multifaceted Pulmonary T Cell Immunity by Combination Adjuvants. Cell Rep. Med. *1*, 100095.

73. Omokanye, A., Ong, L.C., Lebrero-Fernandez, C., Bernasconi, V., Schön, K., Strömberg, A., Bemark, M., Saelens, X., Czarnewski, P., and Lycke, N. (2022). Clonotypic analysis of protective influenza M2e-specific lung resident Th17 memory cells reveals extensive functional diversity. Mucosal Immunol. *15*, 717–729.

74. Domenech, A., Slager, J., and Veening, J.W. (2018). Antibiotic-Induced Cell Chaining Triggers Pneumococcal Competence by Reshaping Quorum Sensing to Autocrine-Like Signaling. Cell Rep. *25*, 2390–2400.e3.

75. Gallay, C., Sanselicio, S., Anderson, M.E., Soh, Y.M., Liu, X., Stamsås, G.A., Pelliciari, S., van Raaphorst, R., Dénéréaz, J., Kjos, M., et al. (2021). CcrZ is a pneumococcal spatiotemporal cell cycle regulator that interacts with FtsZ and controls DNA replication by modulating the activity of DnaA. Nat. Microbiol. *6*, 1175–1187.

76. Schwinn, M.K., Machleidt, T., Zimmerman, K., Eggers, C.T., Dixon, A.S., Hurst, R., Hall, M.P., Encell, L.P., Binkowski, B.F., and Wood, K.V. (2018). CRISPR-Mediated Tagging of Endogenous Proteins with a Luminescent Peptide. ACS Chem. Biol. *13*, 467–474.

77. Entenza, J.M., Loeffler, J.M., Grandgirard, D., Fischetti, V.A., and Moreillon, P. (2005). Therapeutic effects of bacteriophage Cpl-1 lysin against *Streptococcus pneumoniae* endocarditis in rats. Antimicrob. Agents Chemother. *49*, 4789–4792.

78. Bravo, A.M., Typas, A., and Veening, J.W. (2022). 2FAST2Q: a general-purpose sequence search and counting program for FASTQ files. PeerJ *10*, e14041.

79. Liu, X., Gallay, C., Kjos, M., Domenech, A., Slager, J., van Kessel, S.P., Knoops, K., Sorg, R.A., Zhang, J.R., and Veening, J.W. (2017). High-throughput CRISPRi phenotyping identifies new essential genes in *Streptococcus pneumoniae*. Mol. Syst. Biol. *13*, 931.

80. Haas, K.M., Blevins, M.W., High, K.P., Pang, B., Swords, W.E., and Yammani, R.D. (2014). Aging promotes B-1b cell responses to native, but not protein-conjugated, pneumococcal polysaccharides: implications for vaccine protection in older adults. J. Infect. Dis. *209*, 87–97.

81. Shen, A. (2014). Simplified protein purification using an autoprocessing, inducible enzyme tag. Methods Mol. Biol. *1177*, 59–70.

82. Beshara, R., Sencio, V., Soulard, D., Barthélémy, A., Fontaine, J., Pinteau, T., Deruyter, L., Ismail, M.B., Paget, C., Sirard, J.C., et al. (2018). Alteration of Flt3-Ligand-dependent de novo generation of conventional dendritic cells during influenza infection contributes to respiratory bacterial superinfection. PLoS Pathog. *14*, e1007360.

83. Sorg, R.A., Gallay, C., Van Maele, L., Sirard, J.C., and Veening, J.W. (2020). Synthetic gene-regulatory networks in the opportunistic human pathogen *Streptococcus pneumoniae*. Proc. Natl. Acad. Sci. USA *117*, 27608–27619.

84. Keller, L.E., Rueff, A.S., Kurushima, J., and Veening, J.W. (2019). Three New Integration Vectors and Fluorescent Proteins for Use in the Opportunistic Human Pathogen *Streptococcus pneumoniae*. Genes *10*, 394.

CellPress
OPEN ACCESS

STAR★METHODS

KEY RESOURCES TABLE

REAGENT or RESOURCE	SOURCE	IDENTIFIER
Antibodies		
InvivoMab rat anti-mouse CD4 (GK1.5 monoclonal antibody, Bio X cell)	Euromedex	BX-BE003-1-25MG
InvivoMab rat IgG2b isotype control (LTF-2 monoclonal antibody, Bio X cell)	Euromedex	BX-BE0090-25MG
HRP-conjugated goat anti-mouse IgM (Southern Biotech)	Clinisciences	1020-05; RRID: AB_2794201
HRP-conjugated goat anti-mouse IgG (Southern Biotech)	Clinisciences	1030-05; RRID: AB_2619742
HRP-conjugated goat anti-mouse IgA (Southern Biotech)	Clinisciences	1040-05; RRID: AB_2714213
Rabbit antiserum against LafB	Eurogentec	N/A
HRP conjugate goat-anti-mouse IgG	Promega	Cat#W4021; RRID: AB_430834
HRP conjugate goat-anti-rabbit IgG	Abcam	Cat#AB205718; RRID: AB_2819160
HRP conjugate goat-anti-human IgG	Sigma-Aldrich	Cat#A0170; RRID: AB_257868
TCRd-PerCP-eFluor710	Thermo Fisher Scientific	46-5711-82; RRID: AB_2016707
CD45-AF700	Biolegend	103128; RRID: AB_493715
CD19-APC-Cy7	Biolegend	115530; RRID: AB_830707
Gr1-APC-Cy7	Biolegend	108424; RRID: AB_2137485
TCRb-BV421	BD biosciences	562839; RRID: AB_2737830
CD90.2-BV510	Biolegend	105335; RRID: AB_2566587
NKp46-biotine	Biolegend	137616; RRID: AB_11219387
CD11b-biotine	Biolegend	101204; RRID: AB_312786
CD11c-biotine	Biolegend	117304; RRID: AB_313773
CD127-PE-Cy7	Thermo Fisher Scientific	25-1271-82; RRID: AB_469649
CD69-PE	Thermo Fisher Scientific	12-0691-81; RRID: AB_465731
CD103-BV711	Biolegend	121435; RRID: AB_2686970
IL-17A-APC	Miltenyi Biotec	130-112-010; RRID: AB_2652362
Bacterial and Virus Strains		
Streptococcus pneumoniae	Laboratory stock, UK Health Security Agency	NCTC 14078
(Other bacterial strains are listed in Supplementary Table S2)	This paper	N/A
Murine-adapted H3N2 influenza A virus	Dr Mustapha Si-Tahar (University of Tours)	strain Scotland/20/74
Human samples		
Blood from anonymous healthy donors from France	French Public Health Code	EFS contract no. NT/18/2016/200
Chemicals, Peptides, and Recombinant Proteins		
D-luciferine	Synchem	CAS:115144-35-9
Wizard Genomic DNA Purification Kit	Promega	Cat#A1120
NucleoSpin Microbial DNA	Macherey-Nagel	Cat#740235.50
Nano-Glo® HiBiT Extracellular Detection System	Promega	Cat#N2420
Flagellin $FliC_{\Delta 174\text{-}400}$	Laboratory production	N/A
Imject™ Alum Adjuvant	ThermoFisher	Cat#77161
PPSV vaccine Pneumovax®	MSD	Pneumovax®
LafB protein	This paper	N/A
YchF protein	This paper	N/A

(*Continued on next page*)

Continued

REAGENT or RESOURCE	SOURCE	IDENTIFIER
PsaA protein	Dr. Cyrille Grandjean from UMR CNRS 6286 in Nantes, France	N/A
Diphteria toxoid	Instituto biologico argentino S.A.I.C	DAM 049
Brefeldin A	Merck	B5936-200UL
Collagenase VIII	Merck	C2139-5G
PMA	Merck	P8139-1MG
Ionomycine calcium salt 1mM	Merck	I3909-1ML
PhytoHemagglutinin-L	Fisher Scientific	15556286
SepMate™	StemCell	85450
1,2-Diacyl-3-alpha-D-glucosyl-sn-glycerol	Avanti	CAS: 2021179-21-3
1,2-Dioleoyl-sn-glycero-3-phospho-rac-(1-glycerol) sodium salt	Sigma	CAS: 67254-28-8
UDP-α-D-Galactose	Merck Millipore	CAS: 137868-52-1
NucleoSpin RNA II kit	Macherey-Nagel	740955.250
Superscript II Reverse Transcriptase	Invitrogen	18064014
High-Capacity cDNA Archive Kit	Applied Biosystems	4368813
Takyon™ Low ROX SYBR	Eurogentec	UF-LSMT-B0710
Desoxyribonuclease I	Sigma-Aldrich	10104159001
Intracellular Fixation & Permeabilization kit	eBiosciences	88-8824-00
TMB	BD Bioscience	555214
Rompun 2% (xylazine)	Centravet	ATC: QN05CM92
Imalgen 1000 (ketamine)	Centravet	ATC: QN01AX03
Isoflurin	Centravet	ATC: QN01AB06
Doxycycline hyclate	TCI	D4116-5G
Streptavidin-BV605	biolegend	405229
Biorad protein quantification kit	Biorad	Cat#5000002
Deposited Data		
Sequencing output (Fastq files)	This paper	PRJNA895037
Experimental Models: Organisms/Strains		
Mouse: C57BL/6J	Janvier Labs	C57BL/6JRj
Mouse: *Rorc(γt)-Gfp*^{TG}	housing	*Rorc(γt)-Gfp*^{TG}
Mouse: *Il17a*$^{-/-}$	housing	*Il17a*$^{-/-}$
Mouse: BALB/c	Janvier Labs	BALB/cJRj
Oligonucleotides		
Oligos for this study (See Table S3)	Sigma or Eurogentec	N/A
Recombinant DNA		
pLIBT7_A_lafB-CPDHisOld	This paper	N/A
sgRNA library	Addgene	#170432
pLIBT7_A_ychF-CPDHisOld	This paper	N/A
pPEPZ-sgRNAclone	Addgene	#141090
Software and Algorithms		
Prism v8.0	GraphPad Software	https://www.graphpad.com/
ImageJ v2.0	National Institutes of Health	https://imagej.nih.gov/ij/
R v4.1.1	The R Foundation for Statistical Computing	https://www.r-project.org/
Illustrator CC	Adobe	https://www.adobe.com
2FAST2Q (v.2.4.1)	NA	https://veeninglab.com/2fast2q
FlowJo	FlowJo	https://www.flowjo.com

CellPress
OPEN ACCESS

RESOURCE AVAILABILITY

Lead contact

Further information and requests for resources and reagents should be directed to and will be fulfilled by the lead contact, Jan-Willem Veening (jan-willem.veening@unil.ch).

Materials availability

The sgRNA library is available through Addgene (#170432). The generated rabbit antiserum against LafB may be available from the lead contact under a material transfer agreement.

Data and code availability

- The fastq files generated from sequencing are uploaded to the Sequence Read Archive on NCBI with accession number PRJNA895037.
- This work did not use or generate new code.
- Any additional information required to reanalyze the data reported in this paper is available from the lead contact upon request.

EXPERIMENTAL MODELS AND SUBJECT DETAILS

Bacterial strains and culture conditions

S. pneumoniae strains were grown in liquid semi-defined C+Y medium, pH = 6.8[74] at 37C from a starting optical density (OD_{600nm}) of 0.01 until the appropriate OD. Transformation of *S. pneumoniae* was performed as described previously.[33] Transformants were selected on Columbia agar with 5% sheep blood with antibiotics (100 μg/ml spectinomycin, 250 μg/ml kanamycin, 1 μg/ml tetracycline, 40 μg/ml gentamycin, 0.05 μg/ml erythromycin). *E. coli* strains were grown with LB medium or LB agar with appropriate concentrations of antibiotics (100 μg/ml ampicillin, 100 μg/ml spectinomycin, or 50 μg/ml kanamycin). All strains, plasmids and primers used are listed in Tables S2 and S3 within the supplementary information.

Mouse models

Mice experiments complied with national, institutional and European regulations and ethical guidelines, and were approved by the Institutional Animal Care and Use Committee (animal facility agreement D59-350009, Institut Pasteur de Lille, protocol reference: APAFIS#16966, 201805311410769_v3). Six to eight weeks old male C57BL/6JRj, *Rorc(γt)-Gfp*^{TG}, *Il17a*$^{-/-}$ mice were purchased from Janvier Laboratories (Saint Berthevin, France) or bred and maintained in individually ventilated cages (Innorack® IVC Mouse 3.5) and handled in a vertical laminar flow biosafety cabinet (Class II Biohazard, Tecniplast). Male mice were used since they are larger and can better accommodate the volume of instillation of viral and bacterial inoculum than females. All infections were performed in an animal biosafety level 2 facility. For depletion of $CD4^+$ cells, mice received an intraperitoneal injection of 200 μg of GK1.5 monoclonal antibody (rat anti-mouse CD4, Bio X cell) or control isotype on day 34.

Murine superinfection assays

Infections were performed by intranasal (i.n.) route in mice that were previously anesthetized by intraperitoneal (i.p.) injection of 1.25 mg of ketamine and 0.25 mg of xylazine in 200 μL of PBS. Male C57BL/6JRj mice were infected i.n. on day 0 with 50 plaque-forming units (PFU) of the pathogenic murine-adapted H3N2 influenza A virus strain Scotland/20/74 in 30 μL of PBS as previously described.[34] On day 7, mice were infected i.n. with *S. pneumoniae* strains using 5×10^4 CFU of the frozen working stocks diluted in 30 μL of PBS or CRISPRi library using 1.5×10^5 CFU. For CRISPRi experiments, doxycycline (5mg/kg in 200 μL PBS) or PBS (200 μl) were injected intraperitoneally (i.p.) at 1h before and 9 h after *S. pneumoniae* infection. At 24 h post-pneumococcal infection, mice were euthanized by i.p. injection of 5.47 mg of sodium pentobarbital. Lungs and spleen were collected in 1 ml of PBS, homogenized with a T-25 digital Ultraturrax® (IKA) to evaluate CFU count or extract genomic DNA. In some experiments, mouse survival and weight were recorded every day for 10 days after *S. pneumoniae* infection.

Human samples

Blood samples obtained from healthy donors from France to prepare plasma. Blood donation in France is an act of citizenship, solidarity and freedom, and always conducted under strict anonymity by the "Etablissement Français du Sang (EFS ''Nord de France'', Lille). EFS is the French blood establishment, the sole civil operator of blood transfusion in France. Data on age, sex, ancestry, race, ethnicity, and socioeconomic status are thus not collected. Written informed consents for the use of blood for research objectives were obtained from the donors under EFS contract no. NT/18/2016/200 with respect to Decree no. 2007-1220 (articles L1243-4, R1243-61 and following) dated August 10, 2007, of the French Public Health Code. The use of human samples was approved by the French Ministry of Education and Research under the agreement DC 20152575.

METHODS DETAILS

Phase contrast and fluorescence microscopy

S. pneumoniae cells were grown in C+Y medium pH = 6.8 at 37°C to an OD_{595nm} = 0.1 without any inducer and diluted 100-fold in fresh C+Y medium supplemented with 100 μM IPTG. After 1 h of incubation at 37°C in a 5% CO_2 incubator, bacteria were harvested from 1 ml culture by centrifugation at 8000 g, 2 min. The pellet was resuspended in 50 μl PBS, and 0.5 μl of the suspension was spotted onto a PBS agarose pad on microscope slides. Visualization of GFP was performed as described previously.[75]

Split-luciferase HiBiT-tag detection system assay

The assay was performed with the Nano-Glo® HiBiT Extracellular Detection System (Promega). The gene sequence encoding the HiBit tag was inserted to the 5' or 3' end of *lafB* coding sequence by cloning, and the HiBit-tagged *lafB* gene was driven by an IPTG inducible promoter and introduced into the chromosome of *S. pneumoniae* Δ*lafB* mutant. Construction of the mutants is described in the supplementary methods. Note that *lafB* is also known as *cpoA*.[37] The HiBit tag is an 11 amino acid peptide, which can bind to a larger subunit and form a complex with luciferase activity.[76] In this assay, the LgBit subunit can be added into the reaction mixture, but it cannot go through the membrane. So, only when the HiBit tag is exposed to the outside of the cell membrane, luminescence signal can be detected. The *S. pneumoniae* mutants carrying N- or C-terminal Hibit tagged LafB were grown in C+Y acid medium, pH = 6.8, at 37°C until OD600 = 0.3. The culture was then diluted 1:10 into fresh C+Y acid medium with or without 1 mM IPTG for the induction of protein expression. When the OD600 of bacterial culture reached 0.3, the culture was split into two groups: one group was the lysed cell group, in which the bacteria were lysed by addition of 16 μg/ml phage lysin cpl-1,[77] and the other group was the intact cell group, without any lysis step performed. The luciferase assay was performed according to the manufacturer's instructions with the lysed and intact cells. 50 μl of bacterial culture was mixed with 50 μl of reaction reagent of the kit in a black 96-wells plate. Bioluminescence was quantified on a Tecan Infinite 200 PRO luminometer at 37°C. Bioluminescence was measured right after the reagent addition. Four replicates for each condition were performed.

Bacterial genomic DNA extraction and CRISPRi-seq

Lung homogenates were mixed with deoxyribonuclease I (10 μg/mL, Sigma-Aldrich) for 10 min at room temperature and filtered through 100 μm meshes. The filtrate underwent centrifugation at 16,000 *g* and the pellet was used for bacterial gDNA extraction using the NucleoSpin Microbial DNA kit (Macherey-Nagel). For bacterial lysis, 6 cycles of 45 s agitation at a speed of 6 m/s in a FastPrep-24™ homogenizer (MP Biomedicals) were used. DNA was quantified in a NanoDrop spectrophotometer (ThermoFisher) The gDNA was used as template in the one-step PCR to prepare the amplicon libraries for Illumina sequencing as described.[33] Sequencing was performed on an Illumina MiniSeq platform using a 54 dark cycle custom recipe.[33] Raw sgRNA counts were obtained from the fastq files using 2FAST2Q (v.2.4.1) with default settings (PHRED score of minimally 30 and 1 mismatch allowed).[78] Mouse samples PBS 1 and 6, and DOX 1, 5 and 6 were excluded from downstream analyses, on grounds of low pool diversity even without CRISPRi induction (PBS 6), and bottleneck effects (PBS 1, DOX 1, 5, 6). Samples were excluded if >5% of the strains dropped out of the pool without CRISPRi induction, or if the estimated bottleneck size was smaller than three times the pool diversity. Bottleneck sizes were estimated as before,[34] with pneumococcal generation time assumed to be 108 min, time of growth 24h, and the total population size at the start 1.5×10^6 CFU. Differential fitness analyses were performed using DESeq2 (v.1.34.0) in R (v.4.1.1), with hypothesis testing threshold values of an absolute $\log_2$FC>1 and alpha<0.05.

LafB synthetic lethal screening by CRISPRi-seq

A *lafB* knockout strain (VL4017) was constructed in the background of Plac-*dcas9* containing strain DCI23[79] as described in the supplementary methods. The pneumococcal sgRNA library (Addgene #170432) was transformed into the resulting strain. Genome-wide fitness quantification via CRISPRi-seq was then performed in both the wild-type and the *lafB* deletion mutant in parallel. Treatment of the libraries was performed as described before.[34] Specifically, the induction treatment with 1 mM IPTG lasted for 21 generations in C+Y medium, and the control group without induction was set up. The bacteria were collected after treatment followed by genomic DNA isolation. CRISPRi-seq was performed as described previously.[33] Raw sgRNA counts were obtained from the fastq files using 2FAST2Q (v.2.4.1) with default settings.[78] Differential fitness analyses were performed using DESeq2 (v.1.34.0) in R (v.4.1.1), with hypothesis testing threshold values of an absolute $\log_2$FC>1 and alpha<0.05.

Mice vaccination

Mice were vaccinated by the intranasal (i.n.) or subcutaneous (s.c.) route at days 0 and 14. A single vaccine dose per animal contained 20 μg LafB in combination with flagellin $FliC_{\Delta174\text{-}400}$ (2.5 μg) for intranasal vaccination (30μl) or Imject™ Alum (ThermoFisher) for subcutaneous vaccination (100μl). The PPSV vaccine, i.e. Pneumovax® from MSD was used ($^1/_6$ human dose/mice). This represents a dose of 4.17 μg of each capsular polysaccharide per animal (including the serotype 2 capsule produced by the strain D39V). This high dose was chosen to promote optimal anti-capsule antibody response. Other studies have used 1/5th to 1/200th of the human dose.[16,80] For LafB, the dosage was based on similar doses than for other antigens used in vaccination studies. Usually, 10 to 50 μg of antigens (molecular mass between 30-60 KDa) are used in each dose of vaccination experiments in mice. In our study, LafB that is a 40KDa antigen was used at dose of 20 μg per vaccination. Intranasal vaccination was performed under slight anesthesia by gaseous isoflurane (Axience). Antibody and T cell responses were analyzed on blood, spleen, lung and MdLN at day 28 or at day 35, *i.e.*, 7 days after the influenza virus infection.

CellPress
OPEN ACCESS

Antigen-specific immune responses

LafB-, YchF-, PsaA- or Diphteria toxoid (DT)-specific antibodies in serum were assessed by ELISA. Plates were prepared by absorption of LafB, YchF, PsaA or DT (1 μg/ml in carbonate buffer), overnight at 4°C on Maxisorp microplates (Nunc), and 1 h blocking at room temperature with 1% dried milk in PBS. ELISA plates were incubated for 1h at room temperature with serial dilutions of the serum samples. Primary antibody binding was revealed with subsequent incubations with HRP-conjugated goat anti-mouse IgG, IgM or IgA (Southern Biotech) and TMB (BD Bioscience); and measured using a microplate reader at 450/570 nm wavelength. LafB-specific T cell responses were analyzed in spleen, MdLN or lungs. Cells (1×10^6) were incubated for 72h with RPMI 1640 with 10% fetal calf serum, 2mM glutamine, 1mM sodium pyruvate, 10mM HEPES, non-essential amino acids, 100U/100μg Penicillin-Streptomycin and stimulated or not with LafB antigen (50 μg/mL) to measure secretion of IL-13, IL-17A, IL-22, or IFN-γ by ELISA.

Flow cytometry analysis

Lungs were digested with collagenase IA (Sigma, 1 mg/ml) and DNase I (Sigma, 40μg/ml) during 15 min at 37°C. Cells were separated on Percoll 20% and stained for TCRd-PerCP-eFluor710, CD45-AF700, CD19-, Gr1-APC-Cy7, TCRb-BV421, CD90.2-BV510, NKp46-, CD11b-, CD11c-BV605, CD103-BV711, CD69-PE or CD127-PE-Cy7 (Becton Dickinson or Biolegend). Cells were incubated 4h with Brefeldin A (10μg/ml), PMA (25ng/ml) and ionomycin (500ng/ml) and processed for intracellular staining using the kit Intracellular Fixation & Permeabilization (eBiosciences) and IL-17A-APC or control isotype (REAfinity, Miltenyi Biotec). Data were collected on a BD LSR Fortessa and analyzed with FlowJo software.

Analysis of plasma and PBMC from healthy individuals

Plasma (n = 127) and whole blood cells (n = 6) were collected from healthy donors. LafB-, PsaA-, and YchF-specific antibodies were analyzed by ELISA as described above using peroxydase-conjugated goat anti-human IgG antibodies (Sigma-Aldrich). PBMC were purified from blood samples using the SepMate™ (StemCell) as described by the manufacturer. PBMC were cultured ($1x10^6$) for 5 days with RPMI 1640 with 10% fetal calf serum (FCS), 2mM glutamine, 1mM sodium pyruvate, 10mM HEPES, non-essential amino acids, 100U/100μg Penicillin-Streptomycin and stimulated or not with LafB (1μg/ml or 10μg/ml) or Phytohemagglutinin (PHA, 1μg/ml) to measure secretion of IFN-γ by ELISA.

Rabbit LafB antiserum

The rabbit antiserum against LafB was produced by Eurogentec with the speedy 28-day program. The protocol uses a non-Freund adjuvant, and the immunization schedule includes 4 injections on days 0, 7, 10 and 19. 100 μg/injection of tag-free LafB protein was used for the immunization. Before the first injection, 1 pre-immune bleed and ELISA were performed to make sure the absence of antibodies against LafB in the naïve rabbit. Then on day 21, 1 medium bleed was performed to test the production of IgG with ELISA, and the final bleed was performed on day 28.

Western blot and immunoblot

To test the antisera of immunized rabbit or mouse. The *S. pneumoniae* strains were grown in 5 ml of acid C+Y medium to OD600 0.3. The cells were harvested by centrifugation at 8000 g, 5 min. The supernatant was removed, and the pellets were resuspended with cold TE buffer (10 ml of 1 M Tris-HCl pH7.5, 2 ml of 0.5 M EDTA pH8, 88 ml of MQ water, to final 100 ml) for 2 times. Resuspend the pellet in 200 μl of TE buffer, and then break down the bacteria by sonication (1s pulse on, 1s pulse off, Amp 40%) until the solution becomes clear. The total protein concentration was quantified with Biorad protein quantification kit (Biorad, Cat. 5000002), and then all the samples were normalized to the same protein concentration by dilution with TE buffer, which was around 1 mg/ml. 100 μl of cell lysate was mixed with 100 μl of 2×SDS loading buffer, and then boiled at 95°C for 10 min. The samples underwent centrifugation at 15,000 g for 5 min, and then 10 μl of each sample was loaded into one well of a 12% SDS-PAGE (Bio-Rad, Cat. 4561046). 5 μl of PageRuler Plus Prestained Protein Ladder (Fisher, Cat.e 26619) was loaded as marker. The protein samples were transferred onto a PVDF membrane. The PVDF membrane with protein samples was blocked with 5% skim milk (PanReac Applichem, A0830) in PBST (PBS pH7.4 with 0.1% Tween-20) under room temperature for 2 h. The antisera of rabbit or mouse was diluted 1:500 in PBST and then added onto the membrane for 1 h incubation at room temperature. The membrane was then washed 3 times, 5 min each time. The secondary antibodies HRP conjugate goat-anti-mouse IgG (Promega, Cat. W4021; 1:2500 dilution in PBST) or HRP conjugate goat-anti-rabbit IgG (Abcam, Cat. AB205718; 1:5000 dilution in PBST) was added onto the membrane incubated with mouse or rabbit antiserum as the first antibody, respectively. The secondary antibody was incubated with the membrane at room temperature for 1 h, followed by 3 times of washing, 10 min each time. Detection is performed using the SuperSignal West Pico Plus Chemiluminescent Substrate (Thermo scientific, Cat. 34579), and the visualization is performed with the FusionCapt Advance FX7 (Witec AG). To test human plasma, purified LafB antigen (500 ng) was loaded on a 4 to 20% SDS-PAGE, transferred to a nylon membrane, and probed with patient plasma (1:100 dilution) overnight at 4°C. The blot was revealed with a horseradish peroxidase-conjugated goat anti-human IgG secondary antibody (1:10,000 dilution, Sigma-Aldrich) 1h at room temperature and visualized with an enhanced chemiluminescence-based detection kit (West Pico PLUS, Thermo Scientific).

Doxycycline stock

Doxycycline hyclate (TCI Europe) stock solutions were prepared in PBS at a concentration of 10 mg/mL, filtered through 0.22 μm sterile membranes, aliquoted and stored at -80°C. Fresh dilutions were prepared from frozen stocks and the doxycycline free base concentration was corrected using the conversion factor 0.8.

Purification of LafB and YchF protein from *E. coli*

The *lafB* and *ychF* genes were cloned with a CPD tag into vector pLIBT7_A and maintained by *E. coli* DH5α. The recombinant vector was transformed into *E. coli* strain BL21 freshly for protein expression. To induce the expression of LafB or YchF protein in *E. coli* BL21, the strain with the recombinant vector was cultured in 500 ml of buffered TB medium to OD600nm ~0.6 at 37°C, 200 rpm. To prepare the buffered TB medium, first make the 10× Phosphate-buffered saline (2.4 g of KH_2PO_4 and 12.5 g of K_2HPO_4 in 1 L MQ water, autoclave at 121°C, 15 min), and then make the TB medium (24 g of tryptone, 48 g of yeast extract, and 10 ml of glycerol in 900 ml of MQ water, autoclave at 121°C, 15 min), and finally 900 ml of TB medium was mixed with 100 ml of the 10× Phosphate-buffered saline to make 1 L of buffered TB.

The culture was chilled to 16°C when reached OD600nm ~0.6, followed by addition of 0.5 mM IPTG (Isopropyl β-d-1-thiogalactopyranoside) to induce the expression of the recombinant protein with CPD tag overnight (for ~14 h). The bacteria were collected by centrifugation at 4°C, 5000 g. The pellets were resuspended with 75 ml of buffer (50 mM Tris-HCl, pH = 7.5, 300 mM NaCl, 5% Glycerol, 25 mM Imidazole, 5 mM 2-mercaptoethanol, 1 mM PMSF, 750 Units of nuclease). *E. coli* cells were lysed by sonication. Cell lysates underwent centrifugation at 18,000 g, at 4°C for 30 min. The supernatant was then collected for protein purification with cobalt beads. The protocol for purification of the CPD tagged protein is similar to the protocol published previously.[81] Specifically, the supernatant was directly loaded onto cobalt beads, followed by washing with buffer (20 mM Tris, 100 mM NaCl) to remove the nonspecific bindings. We then used 25 ml of elution buffer (20 mM Tris, 100 mM NaCl with 2 mM inositol hexakisphosphate (InsP6)) to elute the protein. Addition of InsP6 activates the protease activity of CPD and the tag is cleaved off, so the final purified protein is tag free. The elution of LafB protein was further purified with Heparin column, and a gradient washing was made by mixing with buffer A1 (20 mM Tris, 100 mM NaCl) and buffer B1 (20 mM Tris, 1 M NaCl). The purified LafB was checked by SDS-PAGE (Figure S2A). Protein YchF was purified in similar way, except that the Hi Trap Q HP anion exchange chromatography column was used for further purification.

Biochemical characterization of the LafB glycosylation activity

Reactions were done with PBS as the principal buffer solution. 30 uL total reaction volumes were set up to contain 10 mM lipid mixture consisting of 1 mM MGlcDAG (1,2-Diacyl-3-alpha-D-glucosyl-sn-glycerol, Avanti) and 9 mM DOPG (1,2-Dioleoyl-sn-glycero-3-phospho-rac-(1-glycerol) sodium salt, Sigma) as well as 1 mM UDP-α-D-Galactose (Merck Millipore). Volumes of purified LafB to desired concentration were added to start reactions. Samples were incubated at 28°C for 30 min before being quenched by the addition of Methanol to a final concentration of 80%. Samples were flash frozen and kept at -80°C until analysis by mass spectrometry.

Bacterial colonization

For quantification of bacteria, lungs and spleen were collected 13 days after infection and homogenized in PBS. Viable counts (colony forming unit [CFU]) were determined by plating serial dilutions onto 5% blood-agar plates.

Viral RNA quantification

Total RNA was extracted with the NucleoSpin RNA II kit (Macherey-Nagel, Duren, Germany). For H3N2 RNA detection, 500 ng of total lung RNA were reverse transcribed with Superscript II Reverse Transcriptase (Invitrogen) in the presence of IAV specific primers targeting the segment 7 which encodes the matrix protein 1 (M1) (5' TCTAACCGAGGTCGAAACGTA 3'). The cDNA was amplified by Taqman real-time PCR using Taqman probe FAM-TTTGTGTTCACGCTCACCGTGCC-TAMRA with forward primer: AAGACCAATC CTGTCACCTCTGA and reverse primer: CAAAGCGTCTACGCTGCAGTCC. A plasmid coding the M1 gene was serially diluted to establish a standard curve (Ct values / plasmid copies). Equivalent of 12.5 ng of total lung RNA was thoroughly used to determine the level of M1 RNA in the lung of infected animals by absolute quantification.[82]

Proinflammatory gene expression

Total RNA was extracted with the NucleoSpin RNA II kit (Macherey-Nagel, Duren, Germany). Total RNA was reverse-transcribed with the High-Capacity cDNA Archive Kit (Applied Biosystems). cDNA was amplified using Takyon™ Low ROX SYBR (Eurogentec). Relative mRNA levels were determined by comparing (a) the cycle thresholds (Ct) for the gene of interest and 2 calibrator genes (ΔCt), *Actb* and *B2m*, and (b) 2–ΔCt values for vaccinated group compared with mock group. The specific primers are CGTCATCCATGGC GAACTG / GCTTCTTTGCAGCTCCTTCGT (*Actb*), TGGTCTTTCTGGTGCTTGTC /GGGTGGCGTGAGTATACTTGAA (*B2m*), CCCTCAA CGGAAGAACCAAA / CACATCAGGTACGATCCAGGC (*Cxcl2*), CTCCAGAAGGCCCTCAGACTAC / GGGTCTTCATTGCGGTGG (*Il17a*), GTTCTCTGGGAAATCGTGGAAA / GTTCTCTGGGAAATCGTGGAAA (*Il6*), and TCAGCAACAGCAAGGCGAAA / CCGCTTCCTG AGGCTGGAT (*Ifng*).

CellPress
OPEN ACCESS

Strain construction

Parent strains for IPTG- or tet-inducible systems

The prsA-lacI-GmR or prsA-lacI-tetR-GmR fragments were amplified from *S. pneumoniae* strain D-LT-PEP9Ptela[83] with primers OVL1694 and OVL1695. The fragments were then transformed into *S. pneumoniae* and select with Columbia blood agar with 1 μg/ml tetracycline.

Gene deletions

Erythromycin resistant marker (eryR) was used as the selection marker for all the deletion mutants in this study. To delete *lafB* gene (SPV_0960), upstream and downstream of *lafB* coding regions were amplified with OVL4184/OVL4185 and OVL4180/4181 oligo pairs, respectively. The DNA sequence containing the coding sequence and ribosome binding site of eryR was amplified with OVL2933/OVL2934. The three amplified upstream, downstream and eryR fragments were then assembled by Golden Gate Assembly using BsaI as the restriction enzyme. The product was then transformed into *S. pneumoniae* and selected with Columbia blood agar with 0.5 μg/ml erythromycin. Deletion of cps locus was performed with the same strategy, and the oligo pairs to amplify the upstream and downstream homologous arms were OVL4610/OVL4611 and OVL4608/OVL4609, respectively.

Complementary strains

The complementary strain of *lafB* was made by introducing an ectopic *lafB* driven by its native promoter on ZIP locus of *S. pneumoniae*.[84] The upstream locus of ZIP locus with a spectinomycin resistant marker was amplified from pPEPZ[84] with OVL3252/OVL3253, and the downstream of the ZIP locus was amplified from pPEPZ with OVL3254/OVL3255. The two acquired fragments were then digested with *BsmBI*. The promoter and coding region of LafB was amplified from the genomic DNA of *S. pneumoniae* D39V with OVL4441 and OVL4442, followed by *BsaI* digestion. Then the three digested fragments were ligated. The ligation product was then transformed into *S. pneumoniae* and the transformants were selected with Columbia blood agar with 100 μg/ml spectinomycin. As a control for the *lafB* complementary strain, the empty pPEPZ was transformed into *S. pneumoniae* and the selection was performed in the same way.

GFP fusion strains

In this study, a C-terminal and N-terminal GFP fused LafB were constructed both driven by an IPTG-inducible promoter at the ZIP locus. To make the N-terminal version of the fusion, we first amplified 3 fragments. The first was a DNA fragment with the upstream of ZIP, spectinomycin resistant marker specR, Plac promoter, and the msfGFP. The fragment was amplified from pASR108[84] with oligos OVL1841/OVL5845. The second fragment was the LafB coding region without start codon and was amplified from genomic DNA of *S. pneumoniae* D39V with oligos OVL5846/OVL5847. The third fragment was the downstream of ZIP locus and was amplified from pASR108 with oligos OVL5851/OVL3255. The three fragments were digested with *BsmBI*, followed by ligation. The ligation product was transformed into *S. pneumoniae* and 100 μg/ml spectinomycin was used for selection. The C-terminal version of fusion was constructed in a similar way, whereas the oligo pairs OVL1841/OVL5849, OVL5850/OVL5853, OVL5851/OVL3255 were used for amplification of the three fragments.

IPTG-inducible HiBiT-tagged lafB mutant

Both N- and C-terminal HiBiT-tagged LafB were constructed at the CIL locus[84] under an IPTG-inducible promoter. Firstly, an IPTG-inducible *lafB* was inserted at the CIL locus, and the produced strain was VL4018. To construct VL4018, three fragments were acquired. The first fragment containing upstream of CIL locus and kanamycin resistant marker was amplified from pASR105 with OVL3318/OVL3371, followed by *NheI* digestion. The second fragment with Plac-*lafB* was amplified from VL4007 with OVL1754/OVL1225, followed by *XhoI* and *NheI* double digestion. The third fragment with downstream of the CIL locus was amplified from pASR105 with oligos OVL925/OVL3321, followed by *XhoI* digestion. The three digested fragment was then ligated and transformed into *S. pneumonie* VL333 to construct VL4018.

To make the HiBiT-tagged *lafB* on N terminal, two fragments were amplified, *BsmBI* digested and ligated, followed by transformation and selection with 150 μg/ml kanamycin. The first fragment containing upstream of CIL locus, kanamycin resistant marker, and IPTG inducible promoter was amplified from VL4018 with OVL6063/OVL3318. The second fragment containing hibit-tagged *lafB* and downstream of CIL locus was amplified from VL4018 with OVL6064/OVL3321. The C terminal HiBiT-tagged LafB was constructed in a similar way, but OVL3318/6065 and OVL6066/OVL3321 were used to amplify the two fragments from VL4018, respectively.

Construction of the CRISPRi libraries

The plasmids with the sgRNA pool were purified with an *E. coli* library (Addgene #170432), and then transformed into different *S. pneumoniae* strains as well described previously.[84]

Construction of luciferase reporter strain (VL2255)

This strain was constructed based on VL2212.[34] The sgRNA targeting *luc* gene was cloned into vector pPEPZ-sgRNAclone (Addgene #141090) as described previously,[84] and the produced plasmid was named as pPEPZ-sgRNAluc. The oligos for annealing of the spacer sequence of sgRNAluc were OVL1020/OVL1021. The pPEPZ-sgRNAluc was then transformed into VL2212 and selected with 100 μg/ml spectinomycin on Columbia agar plates.

Construct the CPD-tagged LafB protein expression plasmid

The *lafB* gene was cloned into the plasmid pLIBT7_A_CPDHisOld for tagging and expression. The *lafB* gene fragment was amplified from genomic DNA of *S. pneumoniae* D39V with two oligos OVL4449/OVL4450, while the backbone of plasmid pLIBT7_A_CPDHisOld was amplified with two oligos "STM121_Bsalins_rev_notag" and "CPDHis_NEW_forward_with_pIDC_overhang". The two fragments were then assembled by Golden Gate Assembly with *BsaI* as the restriction enzyme. The product was transformed into chemically competent *E. coli* DH5α, and the transformants were selected on LB agar with 100 μg/ml ampicillin.

The successfully cloned plasmid "pLIBT7_A_lafB-CPDHisOld" was confirmed by sanger sequencing. For induction of protein expression, the plasmid was transformed into *E. coli* BL21 freshly.

Construction of CRISPRi mutants targeting cozE and divIB

The sgRNAs targeting *cozE* and *divIB* were cloned into vector pPEPZ-sgRNAclone (Addgene #141090) as described previously.[84] Oligos with the spacer sequences targeting *cozE* and *divIB* were OXL812/OXL813 and OXL814/OXL815, respectively. The pPEPZ-sgRNA vectors with the sgRNAs were then transformed into VL4017 and selected with 100 μg/ml spectinomycin on Columbia agar plates.

Antisera production in rabbit used for western blotting

100 μg/injection of protein was used to raise antibodies in one rabbit, and in total 4 injections were performed on day 0, 7, 10, 19, following the Speedy 28-Day program of Eurogentec. The produced antiserum from the immunized rabbit was shown to be immunogenic against, and specific for pneumococcal LafB by Western blotting.

QUANTIFICATION AND STATISTICAL ANALYSIS

Data analyses were performed with GraphPad Prism (v8.0) and R (v4.1.1). Data shown in plots are averages of at least 3 replicates with SEM. For animal infection assays, at least 5 mice were used for each group, and differences were determined using the Mann-Whitney U test for comparing two groups, Kruskal-Wallis test with Dunn's post-analysis for comparing multiple groups. p values were stated in the figure legends.

ADDITIONAL RESOURCES

No additional resources.

DATA AND MATERIALS AVAILABILITY

All data are available in the main text or the supplementary materials. CRISPRi-seq data are available at NCBI Sequence Read Archive: PRJNA895037.

Cell Host & Microbe, Volume *32*

Supplemental information

A conserved antigen induces respiratory Th17-mediated broad serotype protection against pneumococcal superinfection

Xue Liu, Laurye Van Maele, Laura Matarazzo, Daphnée Soulard, Vinicius Alves Duarte da Silva, Vincent de Bakker, Julien Dénéréaz, Florian P. Bock, Michael Taschner, Jinzhao Ou, Stephan Gruber, Victor Nizet, Jean-Claude Sirard, and Jan-Willem Veening

Supplementary Materials for

A conserved antigen induces respiratory Th17-mediated broad serotype protection against pneumococcal superinfection

Xue Liu, Laurye Van Maele, Laura Matarazzo, Daphnée Soulard, Vinicius Alves Duarte da Silva, Vincent de Bakker, Julien Dénéréaz, Florian P. Bock, Michael Taschner, Jinzhao Ou, Stephan Gruber, Victor Nizet, Jean-Claude Sirard, Jan-Willem Veening

Corresponding authors: jean-claude.sirard@inserm.fr, jan-willem.veening@unil.ch

Lead author: Jan-Willem Veening

Supplementary Figures

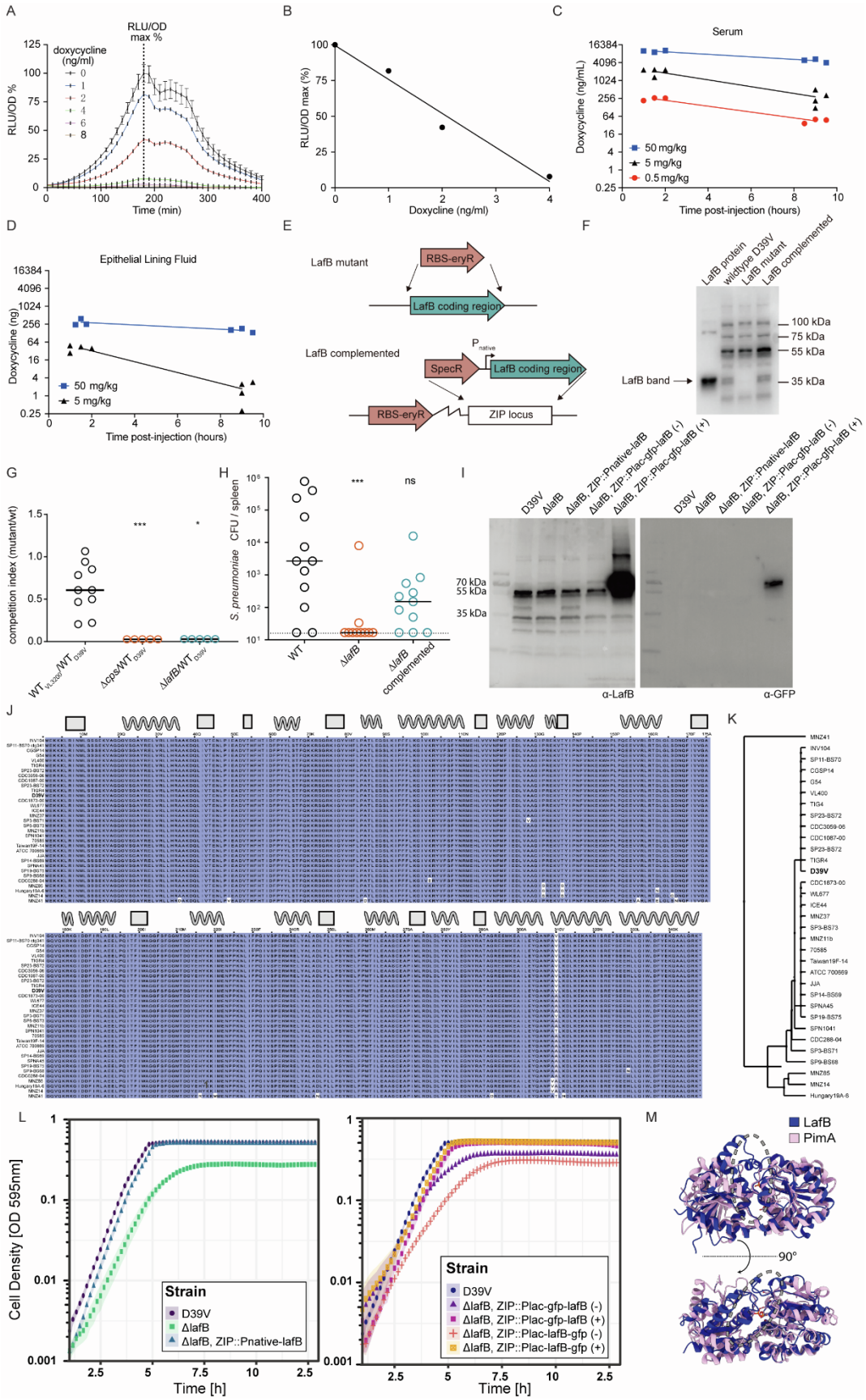

Figure S1. LafB is highly conserved in S. pneumoniae and important for survival in the host, related to figure 1. (A-D) Doxycycline induces *in vitro* and *in vivo* CRISPRi in a dose-dependent manner. Pneumococcal strain VL2255 was constructed that constitutively expresses firefly luciferase (*luc*), has an sgRNA targeting *luc* and a doxycycline-inducible dCas9. (**A-B**) VL2255 was grown in THYB supplemented with D-luciferin at the indicated concentrations of doxycycline. Luminescence (RLU) and cell density (OD) were measured every 10 minutes in a microplate reader. (**A**) Doxycycline gradually decreases the luminescence of VL2255 strain. Data is presented as a percentage of luminescence compared to the control, *i.e.,* no doxycycline (RLU/OD max %). Mean and SD of two replicates. (**B**) The normalized luminescence at the peak (RLU/OD) has a linear correlation with doxycycline concentration. Data are representative of 1 out of 3 experiments. (**C-D**) C57BL/6 mice (n = 3-4) were injected intraperitoneally with 0.5, 5, or 50 mg/kg of doxycycline, and serum and bronchoalveolar lavages (that represent the epithelial lining fluid or ELF) were sampled at 1.5 h and 9 h. VL2255 was grown in THYB, 10% normal mouse serum, D-luciferin and the various concentrations of serum or lavages from doxycycline-injected animals. (**C**) Concentration of doxycycline in serum. (**D**) Amount of doxycycline in ELF. Data are from one experiment. **(E-H) LafB-deficient pneumococci are attenuated for invasive disease.** (**E**) Construction scheme of *lafB* mutant and complemented strain. (**F**) Validation of strains by western blotting using rabbit anti-LafB serum. Purified recombinant tag-free LafB protein (2 ng) was used as a positive control. The cell lysates of wildtype (WT) strain D39V, Δ*lafB* deletion mutant and *lafB* complemented strain as shown in panel (**E**) were loaded with equal amount of total protein. rabbit anti-LafB serum was generated as described in methods, and HRP-conjugated goat-anti-rabbit IgG was used as secondary antibody. (**G**) Spleen data for competition index of mutant compared to wild type D39V. The same analysis as Figure 1c was performed in spleen. Each dot represents the spleen CFU count at day 8 of a single mouse infected with flu at day 0, and a ratio 1:1 of mutant and WT strain at day 7. Capsule deletion mutant (Δ*cps*) was used as control because capsule is a well-known pneumococcal virulence factor. (**H**) Spleen CFU data for single strain infection (mutant vs complemented vs WT). The same analysis as Figure 1d was performed in spleen. Each group included 11-12 mice. There was a significant difference between the wild-type and

ΔlafB strain tested by Kruskal-Wallis test. Note that ectopic expression of *lafB* complemented the phenotype of the *lafB* deletion mutant. (**I-M**) **LafB is a highly conserved membrane-associated pneumococcal GT-B glycosyltransferase.** (**I**) Western blots using anti-LafB serum as well as anti-GFP serum showing the expression of the GFP-LafB protein with and without induction as compared to strains harboring LafB deletion and complementation. GFP-LafB showed the expected size of ~ 65 kDa seemingly lacking any laddering indicative of protein degradation. (**J**) Amino acids sequence alignment of LafB among a selection of relevant *S. pneumoniae* strains spanning a very wide pangenome distribution [18] demonstrating >96% sequence identity. Secondary structure features are indicated above. Background color of each amino acids is based on similarity to the reference sequence of D39V. (**K**) Schematic phylogenetic tree of the LafB proteins in (**J**). (**L**, left) Growth curves showing the growth defect of Δ*lafB* strains and the supplementation by expression of LafB from the ZIP locus under the native *lafB* promoter. Growth curves are the result of triplicate measurements with ribbons denoting the confidence interval of the measurement. (**L**, right) Comparison of growth of strains carrying the GFP-fused LafB proteins with and without supplementation of IPTG in the growth medium demonstrating the supplementation of the LafB phenotype by GFP-tagged LafB proteins. (**M**) Structural comparison of the predicted structure of LafB and the crystal structure of PimA (PDB: 2GEK). GDP as present in PimA crystal structure was left visible for illustration of substrate binding pocket. Backbone structure of both proteins shows good alignment showing the relation between the protein families with the notable divergence of the active site cleft (indicated by grey dashed oval) as expected due to the different substrate specificities of both proteins.

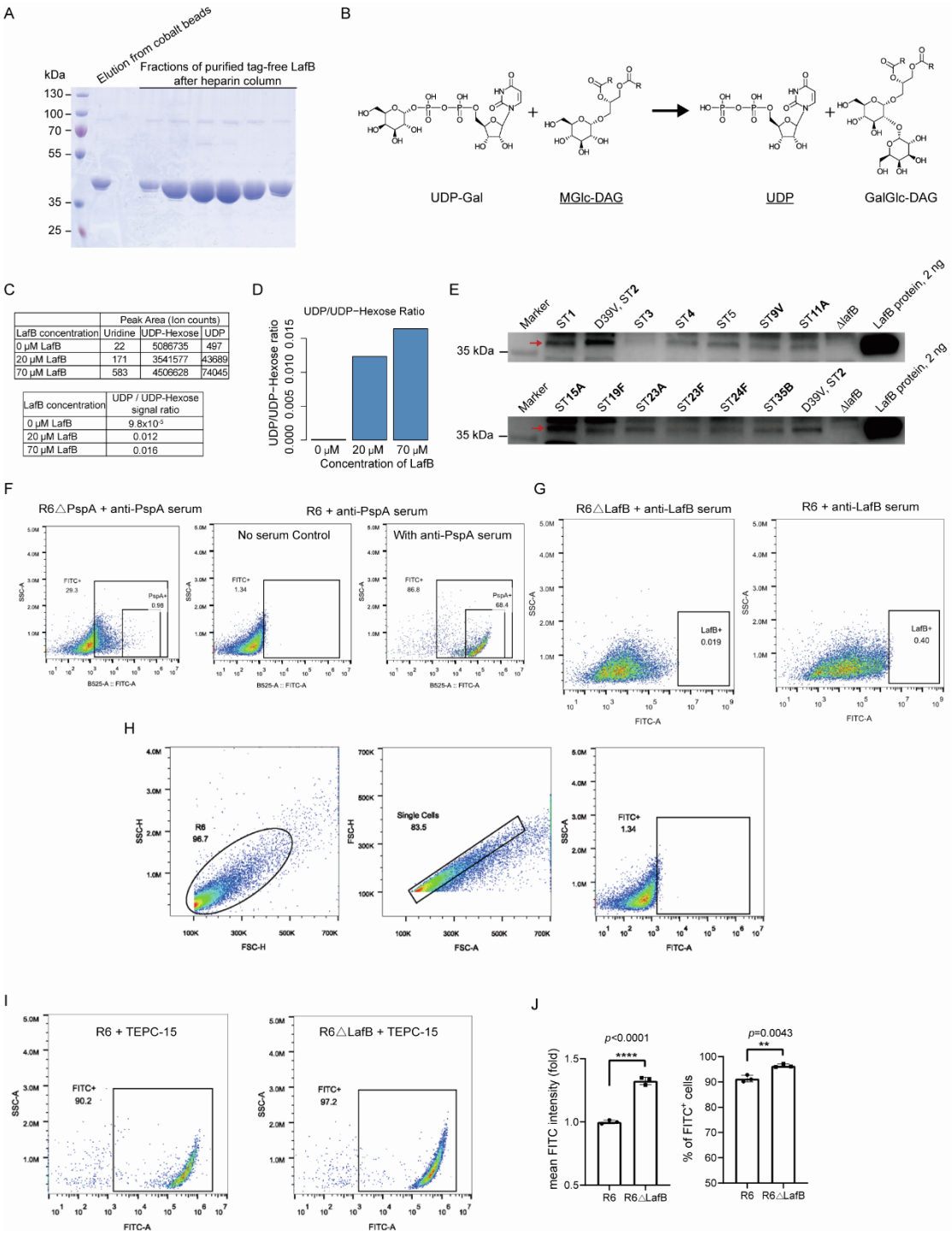

	Peak Area (Ion counts)		
LafB concentration	Uridine	UDP-Hexose	UDP
0 μM LafB	22	5086735	497
20 μM LafB	171	3541577	43689
70 μM LafB	583	4506628	74045

LafB concentration	UDP / UDP-Hexose signal ratio
0 μM LafB	9.8×10^{-5}
20 μM LafB	0.012
70 μM LafB	0.016

Figure S2. LafB catalyzes the formation of galactosyl-glucosyl-diacylglycerol and has an intracellular localization, related to Figure 2. (A-E) Purification and biochemical characterization of LafB in *E. coli* and serotype-independent recognition of LafB by serum from LafB-vaccinated mice. *S. pneumoniae lafB* was cloned in plasmid pLIBT7_A with CPD tag [19], and then the vector was transformed into *E. coli* BL21 for expression. LafB expression was induced by 0.5 mM IPTG in TB medium at 16℃ overnight, and then purified

with cobalt beads followed by further purification with heparin column. Note that the CPD-His6 tag was cleaved off during purification. (**A**) Polyacrylamide gel analysis to show the purification of the tag-free LafB. The gel is stained with Coomassie Brilliant Blue. The expected size of tag-free LafB is 40 kDa. (**B**) Schematic of glycosyltransferase reaction of LafB. Underlined compounds were subject to detection via mass spectrometry. UDP-Gal, Uridine-5′-diphosphogalactose; MGlc-DAG, 1,2-diacyl-3-O-(α-D-glucopyranosyl)-sn-glycerol; UDP, Uridine-5′-diphosphate, GalGlc-DAG, 1,2-Diacyl-3-O-[alpha-D-galactopyranosyl-(1->2)-O-alpha-D-glucopyranosyl]-sn-glycerol. (**C**) Mass spectrometry data from LafB reactions. Raw data depicting the total peak area for the indicated chemical species as well as the product to educt signal ratio for the reaction. (**D**) Barplot visualization depicting the product to educt ratio obtained with different concentrations of LafB after incubation. (**E**) Serum from mice vaccinated with LafB adjuvanted with alum were used to probe LafB by immunoblotting. Whole bacterial lysates from the following serotypes 1, 2, 3, 4, 5, 9V, 11A, 15A, 19F, 23A, 23F, 24F and 35B were prepared for immunoblotting. As shown, LafB was recognized in all strains by Western blotting, including non-vaccine serotypes 15A and 24F. **(F-G) LafB is not present on the pneumococcal cell surface.** (**F**) FACS results of anti-PspA serum-treated *S. pneumoniae* R6Δ*pspA* (left) or wild type R6 (right). (**G**) FACS results of anti-LafB serum-treated *S. pneumoniae* R6Δ*lafB* (left) or R6 (right). *S. pneumoniae* R6, R6Δ*pspA* or R6Δ*lafB* were incubated with anti-PspA rabbit serum (1:50) or anti-LafB rabbit serum (1:50) at 4°C for 60 min first. After centrifugation, *S. pneumoniae* cells were incubated with FITC-labeled goat anti-rabbit IgG antibody at 4°C for 60 min and then measured by flow cytometry. The *S. pneumoniae* cells were first gated using a general viable cell gate (FSC-A versus SSC-A). Then the viable cells were gated for single cells (FSC-A versus FSC-H). *S. pneumoniae* incubated with FACS buffer only was set as negative control and used for FITC gating. This experiment shows that while the well-known surface protein PspA indeed is surface-exposed as shown by this flow cytometry assay, LafB is not. **(H-J) LafB is involved in the synthesis of teichoic acids of *S. pneumoniae*.** (**H-I**) Flow cytometry (FACS) results and gating strategy of the labelling of teichoic acids on *S. pneumoniae* R6 or R6Δ*lafB*. (**J**) Quantification of the

relative mean FITC intensity in teichoic acids-labeled *S. pneumoniae* R6 or R6Δ*lafB,* as showed in panel (**I**). Quantification of $FITC^+$ cells in teichoic acids-labeled *S. pneumoniae* R6 or R6Δ*lafB*, as shown in panel (**I**). *S. pneumoniae* R6 or R6Δ*lafB* were incubated with TEPC-15 monoantibody (1:100), which is specific for phosphorylcholine, at 4°C for 60 min first. After centrifugation, *S. pneumoniae* cells were incubated with FITC-labeled rat anti-mouse IgA antibody at 4°C for 60 min and then measured by flow cytometry. The *S. pneumoniae* cells were first gated using a general viable cell gate (FSC-A versus SSC-A). Then the viable cells were gated for single cells (FSC-A versus FSC-H). *S. pneumoniae* incubated with FACS buffer only was set as negative control and used for FITC gating. The mean FITC intensity and $FITC^+$ cells rate was statistic by FlowJo and presented with GraphPad Prism software.

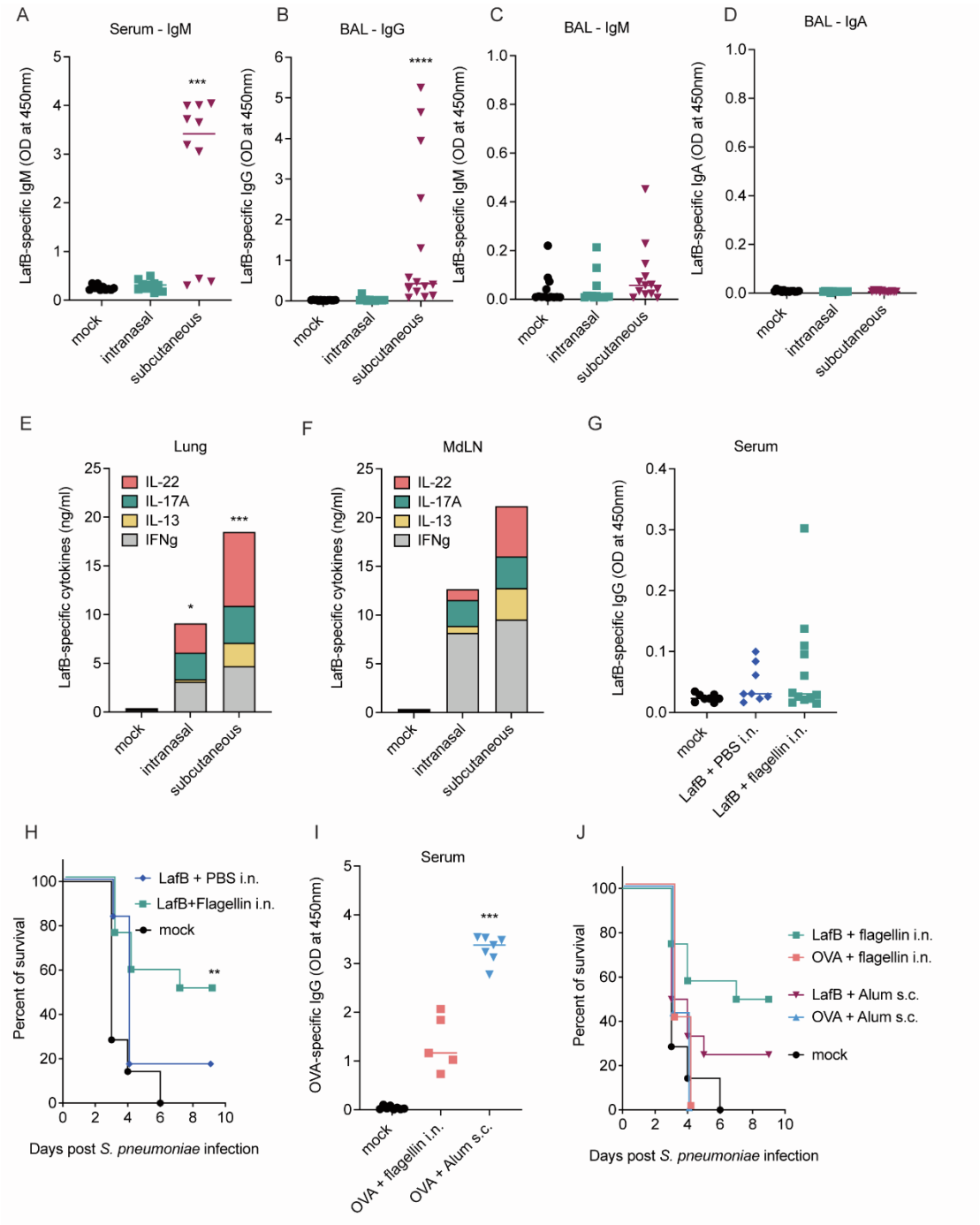

Figure S3. Protection and immune responses induced by intranasal vaccination depends on the LafB antigen and the mucosal adjuvant flagellin, related to Figures 3 and 4. (**A-F**) C57BL/6 mice (n=5-15) were immunized at days 0 and 14 with LafB by intranasal (flagellin-adjuvanted) or subcutaneous (alum-adjuvanted) route, or left untreated (mock) and immune responses were analyzed at day 28. (**A-D**) LafB-specific antibody response. (**A**) Serum IgM and (**B-D**) broncho-alveolar lavage (BAL) LafB-specific IgG (**B**), IgM (**C**) or IgA (**D**) were

determined by ELISA. (**E-F**) LafB-specific T cell response. Lung (**E**) and mediastinal lymph nodes (MdLN) (**F**) cells were stimulated 72h with LafB and cytokine levels in supernatant were determined by ELISA. (**G-H**) LafB-mediated protection requires mucosal adjuvant. C57BL/6 mice (n=7-11) were immunized at days 0 and 14 by intranasal route with LafB alone, LafB adjuvanted with flagellin or left untreated (mock). (**G**) LafB-specific IgG in serum were determined at day 28 by ELISA. (**H**) Vaccinated mice were infected with influenza A virus at day 28 and were challenged at day 35 with 5×10^4 *S. pneumoniae* D39V strain. Protection was assessed by monitoring survival. (**I-J**) Mice were vaccinated with ovalbumin (OVA) as a non-pneumococcal specific control antigen by intranasal (flagellin-adjuvanted) or subcutaneous (alum-adjuvanted) route, or left untreated (mock) and immune responses were analyzed at day 28. (**I**) OVA-specific IgG response in serum at day 28. (**J**) Protection is specific for LafB antigen. Vaccinated mice were challenged as described in panel (**H**). Protection was assessed by monitoring survival. Plots for antibody represent values for individual mice as well as median. Cytokine data are expressed as median. Statistical significance (*$P<0.05$, *** $p<0.001$) was assessed by one-way ANOVA Kruskal-Wallis test with Dunn's correction compared to the mock group. Statistical significance for survival (** $p<0.01$) was assessed by Mantel-Cox test compared to the mock group.

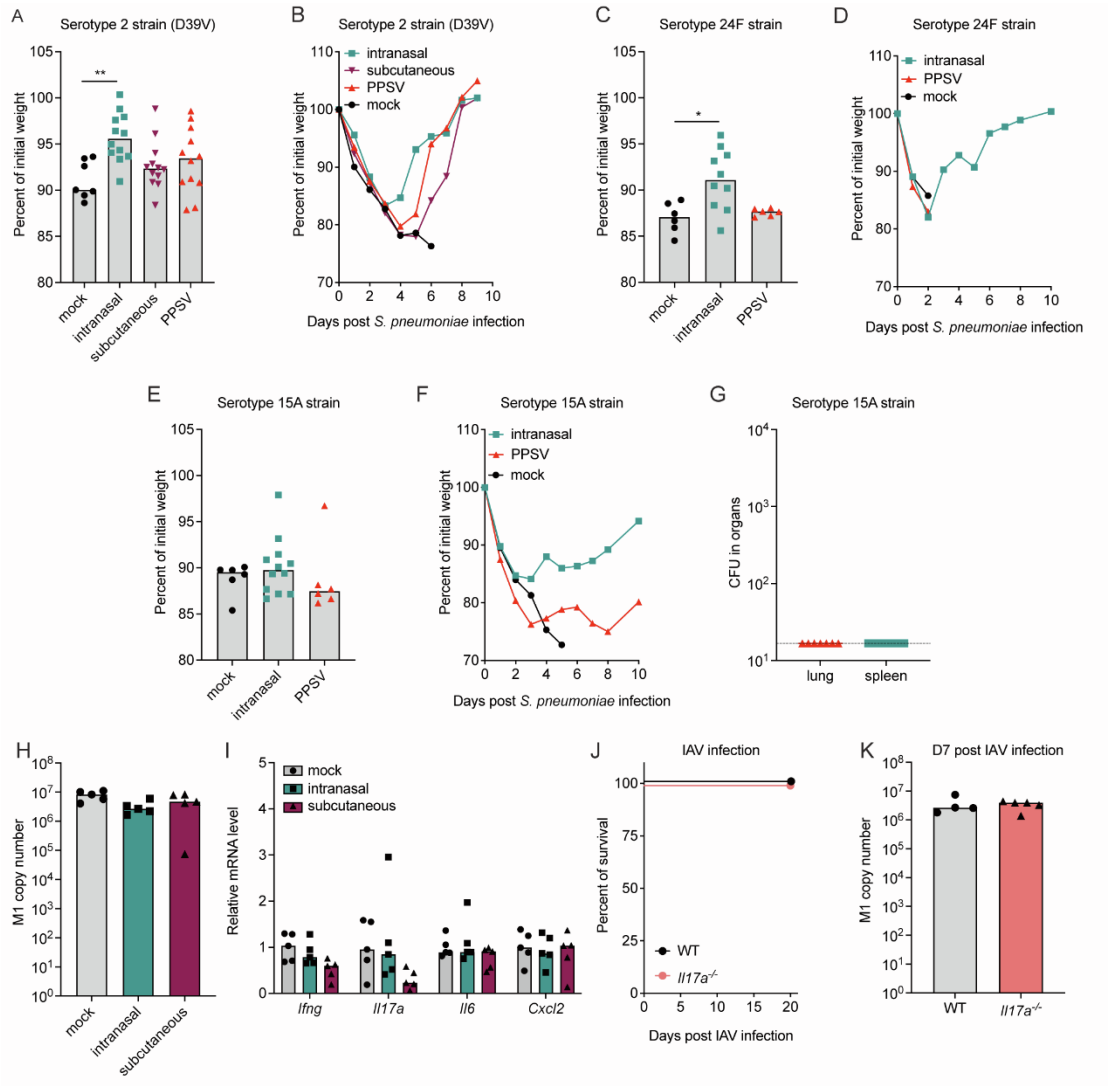

Figure S4. Intranasal vaccination with adjuvanted LafB attenuated the pathology caused by *S. pneumoniae* and led to complete bacterial clearance, related to Figures 3 and 4. (A-G) C57BL/6 mice (n=6-12) were immunized at days 0 and 14 with adjuvanted LafB intranasal (flagellin-adjuvanted) or adjuvanted LafB subcutaneous (alum-adjuvanted) route, a commercial PPSV vaccine, or unvaccinated (mock). Mice were infected with influenza virus at day 28 and with *S. pneumoniae* at day 35 using the strain D39V of serotype 2 (**A-B**, 5×10^4 CFU: 7 mock, 12 PPSV, 12 intranasal, 12 subcutaneous) is representative of 5 experiments), serotype 24F (**C-D**, 10^3 CFU: 6 mock, 6 PPSV, 10 intranasal) is representative of 2 experiments), or serotype 15A strain (**E-G**, 5×10^4 CFU: 6 mock, 6 PPSV, 10 intranasal). (**A, C and E**) Weight loss at day 36 (24 h post-bacterial challenge). Plots represent values for individual mice as well as median. Statistical significance (*P<0.05, ** p<0.01) was assessed by one-way ANOVA Kruskal-

Wallis test with Dunn's correction compared to the mock group. (**B, D and F**) Weight monitoring of the mice during *S. pneumoniae* infection. Median weight of surviving animals are shown. (**G**) Bacterial load at day 49 (i.e., 13 days post-pneumococcal infection) in lung and spleen of surviving mice immunized intranasally with flagellin adjuvanted LafB (n=7 from 10).

(H-I) LafB immunization does not alter the course of lung infection or inflammatory response induced by influenza virus. C57BL/6 mice (n=5) were immunized or left unvaccinated (mock) at days 0 and 14 with LafB by intranasal (flagellin-adjuvanted) or subcutaneous (alum-adjuvanted) route or left unvaccinated (mock). Mice were infected with H3N2 influenza A virus at day 28 and lungs were sampled seven days later (day 35) for gene expression analysis by qPCR. (**H**) Relative viral RNA level (M1 RNA copies/µg RNA) in lung. (**I**) Expression of pro-inflammatory genes in lung. Plots represent values for individual mice as well as median. **(J-K) Absence of *Il17a* expression does not alter nor exacerbate the course of influenza virus respiratory infection**. C57BL/6 (WT) or *Il17a*$^{-/-}$ mice were infected i.n. on day 0 with 50 plaque-forming units (PFU) of the pathogenic murine-adapted H3N2 influenza A virus strain Scotland/20/74 in 30 µL of PBS. (**J**) Survival of mice (4 WT and 7 *Il17a*$^{-/-}$) was monitored for 20 days. (**K**) At day 7 post-IAV infection, lungs (4 WT and 5 *Il17a*$^{-/-}$) were sampled for analysis of viral RNA level (M1 RNA copies/µg RNA) by qPCR. Plots represent values for individual mice as well as median and are from one experiment.

Supplementary Tables

Table S2. Strains and plasmids used in the study, related to STAR Methods.

Strains/Plasmids	Genotype	Reference
S. pneumoniae		
D39V	Serotype 2 strain, wild-type	[20]
R6	Unencapsulated derivative of D39	Veening lab collection
DCI23	D39V, Δ*bgaA*::*Plac-*dcas9*sp (tet^R); Δ*prs1*::PF6-*lacI* (Gm^R)	[21]
VL4181	Serotype 15A strain, wild-type, clinical isolate	This study
VL4182	Serotype 24F strain, wild-type, clinical isolate	This study
VL1310	Serotype 1 strain, wild-type, PMEN28, Sweden^1-28 Clone, clinical isolate	This study
VL1311	Serotype 3 strain, wild-type, PMEN31, Netherlands^3-31 clone, clinical isolate	This study
VL2177	Serotype 4 strain, wild-type, TIGR4	Sven Hammerschmidt group collection
VL1308	Serotype 5 strain, wild-type, PMEN19, Colombia^5-19 Clone, clinical isolate	This study
VL1307	Serotype 9V strain, wild-type, PMEN3, Spain^{9V}-3 clone, clinical isolate	This study
VL1313	Serotype 11A strain, wild-type, clinical isolate	This study
VL3483	Serotype 19F strain, wild-type, clinical isolate	This study
VL3411	Serotype 23A strain, wild-type, clinical isolate	This study
VL1306	Serotype 23F strain, wild-type, PMEN1, Spain^{23F}-1 clone, clinical isolate	This study
VL4304	Serotype 35B strain, wild-type, clinical isolate	This study
VL2212	D39, Δ*prs*1::PF6-*tetR* (Gm^R), Δ*bgaA*:: *Ptet-*dcas9* (tet^R)	[17]
VL2255	D39, Δ*prs1*::PF6-*tetR*(Gm^R), Δ*bga*::Ptet-*dcas9*(tet^R), CIL::P3-*luc* (Kan^R), ZIP::P3-sgRNAluc(Spec^R)	This study
VL3200	D39V, *hlpA*::*hlpA-mKate-eryR*(ery^R)	Veening lab collection
VL3508	D39V, Δ*cps*::*eryR*(ery^R)	[17]
VL3458	D39V, Δ*lafB*::*eryR*(ery^R)	This study
VL3511	D39V, Δ*lafB*:*eryR*(ery^R), ZIP::Plac-empty(Spec^R)	This study
VL3516	D39V, Δ*lafB*:*eryR*(ery^R), ZIP::Pnative-*lafB*(Spec^R)	This study
VL333	D39V, Δ*prs1*::*tetR-lacI* (Gm^R)	This study
VL4008	D39V, Δ*prs1*::*tetR-lacI* (Gm^R), *lafB*::eryR	This study
VL4006	D39V,Δ*prs1*::*tetR-lacI*(Gm^R),ZIP::Plac-msfGFPopt-*lafB*, Δ*lafB*::*eryR*(ery^R)	This study
VL4007	D39V, Δ*prs1*::*tetR-lacI*(Gm^R), ZIP::Plac-*lafB*-msfGFPopt(Spec^R),	This study

	Δ*lafB*::*eryR*(ery^R)	
VL4017	D39V, Δ*prs1*::*tetR-lacI*(Gm^R), Δ*lafB*::*eryR*(ery^R)	This study
VL4018	D39V, Δ*prs1*::*tetR-lacI*(Gm^R), CIL::Plac-*lafB* (Kan^R)	This study
VL4039	DCI23, Δ*lafB*::*eryR*(ery^R)	This study
VL4048	DCI23, ZIP:sgRNA1-1499 (Spec^R)	This study
VL4042	DCI23, Δ*lafB*::*eryR*(ery^R), ZIP:sgRNA1-1499 (Spec^R)	This study
VL4056	D39V, Δ*prs1*::*tetR-lacI* (GmR), Δ*lafB*::*eryR*, CIL::Plac-Hibit-*lafB* (Kan^R)	This study
VL4057	D39V, Δ*prs1*::*tetR-lacI* (Gm^R), Δ*lafB*::*eryR*(ery^R), CIL::Plac-*lafB*-Hibit (Kan^R)	This study
SZU486	D39V, Δ*prs1*::*tetR-lacI*(Gm^R), Δ*lafB*::*eryR*(ery^R), ZIP-sgRNA*cozE*	This study
SZU487	D39V, Δ*prs1*::*tetR-lacI*(Gm^R), Δ*lafB*::*eryR*(ery^R), ZIP-sgRNA*divIB*	This study
SZU1227	R6, Δ*lafB*::*eryR*(ery^R)	This study
SZU1228	R6, Δ*PspA*::*eryR*(ery^R)	This study
E. coli		
DH5a	F$^-$*endA1 glnV44 thi-1 recA1 relA1 gyrA96 deoR nupG purB20* ϕ80d*lacZ*ΔM15 Δ(*lacZYA-argF*)U169, hsdR17($r_K^- m_K^+$), λ$^-$	Veening lab collection
BL21		Stephan Gruber lab collection
Plasmids		
sgRNA pools	pPEPZ-sgRNA1-1499 for *S. pneumoniae* D39V (Spec^R)	Addgene #170432
pLIBT7_A_CPDHisOld	pUCori-rop-lacI-Plac- CPD10His-f1 ori-AmpR (Amp^R)	Stephan Gruber lab collection
pLIBT7_A_lafB-CPDHisOld	pUCori-rop-lacI-Plac-lafB-CPD10His-f1 ori-AmpR(Amp^R)	This study
pPEPZ-sgRNAclone	Addgene # 141090	[17]
pPEPZ-sgRNAluc	with an sgRNA targeting *luc* gene on pPEPZ-sgRNAclone (Spec^R)	This study
pPEPY (pASR105)	Intergration vector at CIL locus (Kan^R)	[16]
pASR108	Intergration vector at ZIP locus with msfGFP (Spec^R)	[16]
pPEPZ	Intergration vector at ZIP locus (Spec^R)	[16]

Amp^R: ampicillin resistant; ery^R: erythromycin resistant; Gm^R: gentamycin resistant; Kan^R: kanamycin resistant; Spec^R: spectinomycin resistant; tet^R: tetracycline resistant

Table S3. Primers used in the study, related to STAR Methods.

Primer name	5'-3'
Make gene deletion mutants	
OVL2933_eryR-F-BsaI	GATCGGTCTCGAGGAATTTTCATATGAACAAAAATATAAAATATTCTCAA
OVL2934_eryR-R-BsaI	GATCGGTCTCGTTATTTCCTCCCGTTAAATAATAGATAACTATTAAAAAT
OVL4180_lafB-dnF-BsaI	gatcggtctcgATAAaaagtgaggtaatctatgcgaatt
OVL4181_lafB-dnR	ccagtaggaatgacccg
OVL4182_lafB-seqF	gactagatgatggaaaaatgcgc
OVL4183_lafB-seqR	tacgcagttctttcaaattttcctg
OVL4184_lafB-upF	ggggaaagtctttaacgtaactc
OVL4185_lafB-upR-BsaI	gatcggtctcaTCCTtaactactattatatcattttctttg
OVL4608_cps-dn-F-BsaI	GATCGGTCTCAATAAgttgtttgaaaaataattttcaaaaattctg
OVL4609_cps-dnR	attatctgataaatcccagtcttcgc
OVL4610_cps-up-R-BsaI	gatcggtctcTTCCTatacattgaacatcttacgattatatcactttttta
OVL4611_cps-upF	ctccctcgtattgtctcaatct
Make complementary strains	
OVL3252_ZIP-upF	GCCAATAAATTGCTTCCTTGTTTTG
OVL3253_ZIPup-R-BsmBI	ccttcgtctcgACTAGTGAATTCTATAAACGCAGAAAG
OVL3254_ZIPdn-F-BsmBI	ccttcgtctcgAGGAAAAATAATGCCGGATCCCT
OVL3255_ZIPdn-R	ATGACACGGATTTTAAGAATAATTCTTTCT
OVL4441_lafBcom-F-BsaI	gatcggtctcCTAGTacatataaaagcatgtgagagactgttgg
OVL4442_lafBcom-R-BsaI	gatcggtctcTTCCTagattacctcacttttttactttctccc
GFP fusions	
OVL1841_pPEPZ_F	ACAAAAGTGTGCTATTCTTTTTATGAGAG
OVL5845_msfGFP-R-BsmBI	tcagcgtctccTTTGTATAGTTCGTCCATGCC
OVL5846_linker-lafB-F	GATCCGTCTCACAAAggatccggatctggtggagaagctgcagctaaaggatcagagaaaaagaaattacgcatcaat
OVL5847_lafB-R-BsmBI	gatccgtctctATTActttctccctaaagcggc
OVL3255_ZIPdn-R	ATGACACGGATTTTAAGAATAATTCTTTCT
OVL5849_pASR108-up-R-BsmBI	gatccgtctcaccatATTTGCCTCCTTAAAGATCTTAATTG
OVL5850_lafB-RBS-F-BsmBI	gatccgtctcgatggagaaaaagaaattacgcatca
OVL5851_msfGFP-linker-F-	gatccgtctcaggatccggatctggtggagaagctgcagctaaaggatcaTCAAAA

BsmBI	GGCGAAGAACTATTCACA
OVL5853_msfGFP-eryR-R-BsmBI	gatccgtctcaTCCTTTATTTGTATAGTTCGTCCATGC
OVL6159_cozEa-F-Nter-BsmBI	gatccgtctcgatcatttcgtagaaataaattatttttttggacc
OVL6160_cozEa-R-Nter-BsmBI	gatccgtctcaCGAGTTActtagctaattctctttctcgttc
OVL6164_cozEa-F-Cter-BsmBI	gatccgtctcgagttatgtttcgtagaaataaattatttttttggac
OVL6165_cozEa-R-Cter-BsmBI	GATCCGTCTCACCAGcttagctaattctctttctcgttct
HiBiT tag fusions	
OVL6063_cil-up-Hibit-R-bsmbI	gatccgtctctACCAGAAATTTTTTTAAACAAACGCCAACCAGAAACcataactactCCTCCTGATCTTAATTGTG
OVL6064_lafB-Hibit-F-bsmbI	GATCCGTCTCACTGGTGGTGGTGGTTCTGGTGGTGGTGGTTCTgagaaaaagaaattacgcatcaatatgt
OVL6065_lafB-Hibit-R-bsmBI	GATCCGTCTCAACCAGAAACAGAACCACCACCACCAGAACCACCACCACCctttctccctaaagcggct
OVL6066_hibit-cil-dn-F-bsmBI	gatcCGTCTCATGGTTGGCGTTTGTTTAAAAAAATTTCTTAATAACTCGAGAAAGTGTAAGCAATTCTG
OVL3318_pASR105_UpF	AAACCTTACTAAAGTATATAATTTAGGC
OVL3371_(pPEPY)-SPV_564*mNeon_R	AATCCGCGTCTCCcatTAATTTTCCTCCTTATTTATTTAGATCTCATGAATTCAATTGTG
OVL1754_LK354	TGGTCTCCGATCGTGTACTG
OVL1225_	GATTGCCCTCTTGTTCAG
OVL925_pPEPY-Linear-R	GGATCCCTCCAGTAACTCGAGAA
OVL3321_pASR105_DoR	ATAAAAACATTCATCATAACCCCC
CRISPRi targeting cozE and divIB	
OXL812_sgRNA-Sp-cozE-F	tataGGTTAAGAGTAAAATTTCTG
OXL813_sgRNA-Sp-cozE-R	aaaccagaaattttactcttaacc
OXL814_sgRNA-Sp-divIB-F	tataTAACTCTTTCAATTCTTCGA
OXL815_sgRNA-Sp-divIB-R	aaactcgaagaattgaaagagtta
Insertion tetR and lacI	
OVL1694_prsA lacI-tetR-GmR FWD	AGGACACACCTGCAGTGCCTTATTATTATTGTCCACTTTCCAAAC

OVL1695_prsA lacI-tetR-GmR REV	AGGACACACCTGCAGTGTATGCTCGAAGATTTCAGCTTGACATT
Construction of LafB protein expression plasmid	
STM121 BsaIins rev notag	acgtatggtctccatggttatatctccttcttaaagttaaacaaaattatttctagaggg
CPDHis NEW forward with pIDC overhang	CTCCGGAATATTAGGTCTCAggatctCTCGCGGGCGGTAAAATACTCC
OVL4449_lafB-TMA-F-BsaI	ctccggaatattaggtctcaCCATggagaaaaagaaattacgcatcaatat
OVL4450_lafB-TMA-R-BsaI	GGCTCAAGCAGTGGGTCTCCATCCctttctccctaaagcggc
Construction of the luciferase reporter strain	
OVL1020_GG-sgRNAluc-F	AAACGGCGCCATTCTATCCTCTAG
OVL1021_GG-sgRNAluc-R	TATACTAGAGGATAGAATGGCGCC
Viral RNA quantification	
Forward primer	AAGACCAATCCTGTCACCTCTGA
Reverse primer	CAAAGCGTCTACGCTGCAGTCC
Proinflammatory gene expression	
Actb-1	CGTCATCCATGGCGAACTG
Actb-2	GCTTCTTTGCAGCTCCTTCGT
B2m-1	TGGTCTTTCTGGTGCTTGTC
B2m-2	GGGTGGCGTGAGTATACTTGAA
Cxcl2-1	CCCTCAACGGAAGAACCAAA
Cxcl2-2	CACATCAGGTACGATCCAGGC
Il17a-1	CTCCAGAAGGCCCTCAGACTAC
Il17a-2	GGGTCTTCATTGCGGTGG
Il6-1	GTTCTCTGGGAAATCGTGGAAA
Il6-2	GTTCTCTGGGAAATCGTGGAAA
Ifng-1	TCAGCAACAGCAAGGCGAAA
Ifng-2	CCGCTTCCTGAGGCTGGAT

References

1. Domenech, A., Slager, J., and Veening, J.-W. (2018). Antibiotic-Induced Cell Chaining Triggers Pneumococcal Competence by Reshaping Quorum Sensing to Autocrine-Like Signaling. Cell Rep. *25*, 2390-2400.e3. 10.1016/J.CELREP.2018.11.007.

2. de Bakker, V., Liu, X., Bravo, A.M., and Veening, J.-W. (2022). CRISPRi-seq for genome-wide fitness quantification in bacteria. Nat. Protoc. *17*, 252–281. 10.1038/s41596-021-00639-6.

3. Gallay, C., Sanselicio, S., Anderson, M.E., Soh, Y.M., Liu, X., Stamsås, G.A., Pelliciari, S., van Raaphorst, R., Dénéréaz, J., Kjos, M., et al. (2021). CcrZ is a pneumococcal spatiotemporal cell cycle regulator that interacts with FtsZ and controls DNA replication by modulating the activity of DnaA. Nat. Microbiol. *6*, 1175–1187. 10.1038/s41564-021-00949-1.

4. Grebe, T., Paik, J., and Hakenbeck, R. (1997). A novel resistance mechanism against beta-lactams in *Streptococcus pneumoniae* involves CpoA, a putative glycosyltransferase. J. Bacteriol. *179*, 3342–3349. 10.1128/jb.179.10.3342-3349.1997.

5. Schwinn, M.K., Machleidt, T., Zimmerman, K., Eggers, C.T., Dixon, A.S., Hurst, R., Hall, M.P., Encell, L.P., Binkowski, B.F., and Wood, K.V. (2018). CRISPR-Mediated Tagging of Endogenous Proteins with a Luminescent Peptide. ACS Chem. Biol. *13*, 467–474. 10.1021/acschembio.7b00549.

6. Entenza, J.M., Loeffler, J.M., Grandgirard, D., Fischetti, V.A., and Moreillon, P. (2005). Therapeutic effects of bacteriophage Cpl-1 lysin against *Streptococcus pneumoniae* endocarditis in rats. Antimicrob. Agents Chemother. *49*, 4789–4792. 10.1128/aac.49.11.4789-4792.2005.

7. Liu, X., Kimmey, J.M., Matarazzo, L., de Bakker, V., Van Maele, L., Sirard, J.-C., Nizet, V., and Veening, J.-W. (2021). Exploration of Bacterial Bottlenecks and *Streptococcus pneumoniae* Pathogenesis by CRISPRi-Seq. Cell Host Microbe *29*, 107-120.e6. 10.1016/j.chom.2020.10.001.

8. Bravo, A.M., Typas, A., and Veening, J.-W. (2022). 2FAST2Q: a general-purpose sequence search and counting program for FASTQ files. PeerJ *10*, e14041. 10.7717/peerj.14041.

9. Liu, X., Gallay, C., Kjos, M., Domenech, A., Slager, J., van Kessel, S.P., Knoops, K., Sorg, R.A., Zhang, J.-R., and Veening, J.-W. (2017). High-throughput CRISPRi phenotyping identifies new essential genes in *Streptococcus pneumoniae*. Mol. Syst. Biol. *13*, 931. 10.15252/msb.20167449.

10. Jirru, E., Lee, S., Harris, R., Yang, J., Cho, S.J., and Stout-Delgado, H. (2020). Impact of Influenza on Pneumococcal Vaccine Effectiveness during *Streptococcus pneumoniae* Infection in Aged Murine Lung. Vaccines *8*, 298. 10.3390/vaccines8020298.

11. Haas, K.M., Blevins, M.W., High, K.P., Pang, B., Swords, W.E., and Yammani, R.D. (2014). Aging promotes B-1b cell responses to native, but not protein-conjugated,

pneumococcal polysaccharides: implications for vaccine protection in older adults. J. Infect. Dis. *209*, 87–97. 10.1093/infdis/jit442.

12. Shen, A. (2014). Simplified protein purification using an autoprocessing, inducible enzyme tag. Methods Mol. Biol. Clifton NJ *1177*, 59–70. 10.1007/978-1-4939-1034-2_5.

13. Beshara, R., Sencio, V., Soulard, D., Barthélémy, A., Fontaine, J., Pinteau, T., Deruyter, L., Ismail, M.B., Paget, C., Sirard, J.-C., et al. (2018). Alteration of Flt3-Ligand-dependent de novo generation of conventional dendritic cells during influenza infection contributes to respiratory bacterial superinfection. PLOS Pathog. *14*, e1007360. 10.1371/journal.ppat.1007360.

14. Sorg, R.A., Gallay, C., Van Maele, L., Sirard, J.-C., and Veening, J.-W. (2020). Synthetic gene-regulatory networks in the opportunistic human pathogen *Streptococcus pneumoniae*. Proc. Natl. Acad. Sci. U. S. A. *117*, 27608–27619. 10.1073/pnas.1920015117.

15. de Bakker, V., Liu, X., Bravo, A.M., and Veening, J.-W. (2022). CRISPRi-seq for genome-wide fitness quantification in bacteria. Nat. Protoc. *17*, 252–281. 10.1038/s41596-021-00639-6.

16. Keller, L.E., Rueff, A.-S., Kurushima, J., and Veening, J.-W. (2019). Three New Integration Vectors and Fluorescent Proteins for Use in the Opportunistic Human Pathogen *Streptococcus pneumoniae*. Genes *10*, 394. 10.3390/genes10050394.

17. Liu, X., Kimmey, J.M., Matarazzo, L., de Bakker, V., Van Maele, L., Sirard, J.-C., Nizet, V., and Veening, J.-W. (2021). Exploration of Bacterial Bottlenecks and *Streptococcus pneumoniae* Pathogenesis by CRISPRi-Seq. Cell Host Microbe *29*, 107-120.e6. 10.1016/j.chom.2020.10.001.

18. Antic, I., Brothers, K.M., Stolzer, M., Lai, H., Powell, E., Eutsey, R., Cuevas, R.A., Miao, X., Kowalski, R.P., Shanks, R.M.Q., et al. (2017). Gene Acquisition by a Distinct Phyletic Group within *Streptococcus pneumoniae* Promotes Adhesion to the Ocular Epithelium. mSphere *2*, e00213-17. 10.1128/mSphere.00213-17.

19. Shen, A., Lupardus, P.J., Morell, M., Ponder, E.L., Sadaghiani, A.M., Garcia, K.C., and Bogyo, M. (2009). Simplified, enhanced protein purification using an inducible, autoprocessing enzyme tag. PloS One *4*, e8119. 10.1371/journal.pone.0008119.

20. Slager, J., Aprianto, R., and Veening, J.-W. (2018). Deep genome annotation of the opportunistic human pathogen *Streptococcus pneumoniae* D39. Nucleic Acids Res. *46*, 9971–9989. 10.1093/nar/gky725.

21. Liu, X., Gallay, C., Kjos, M., Domenech, A., Slager, J., Kessel, S.P. van, Knoops, K., Sorg, R.A., Zhang, J.-R., and Veening, J.-W. (2017). High-throughput CRISPRi phenotyping identifies new essential genes in *Streptococcus pneumoniae*. Mol. Syst. Biol. *13*, 931. 10.15252/msb.20167449.